

## **Response to Reviews – Esurf Manuscript**

### **Effects of seasonal variations in vegetation and precipitation on catchment erosion rates along a climate and ecological gradient: Insights from numerical modelling**

By: Sharma and Ehlers

#### **Response to Associate Editor: Simon Mudd**

Dear Prof. Simon Mudd,

We would like to thank you for agreeing to be the associate editor of our manuscript. We also thank our two anonymous referees and Omer Yetemen for their valuable comments and suggestions. We performed major revisions in our manuscript as per the comments and suggestions by the reviewers. We addressed each comment by the reviewers and believe that the quality of our manuscript is substantially improved and made it more useful to prospective readers. We hope the revised manuscript also meets the referees' expectations and high standard of Esurf. The most important changes are summarized below.

In response to RC1, we revised our manuscript thoroughly in regards of the readability of the figures (e.g., Figs. 2 – 12 except Fig. 3). We extensively revised the results section in order to improve the analysis and interpretation of our model output. We also modified the representation of the results and associated statistical treatments for resolving the specific questions asked in the study (e.g., analysis and interpretation of proportional changes in forcings and response to explore the sensitivities) and plotting the system sensitivities in Figs. 5, 7, and 9. We also added a subsection (section 5.3) in the discussion to account for the consideration of potential time lags in sediment erosion. A new subsection in Appendix (section A2) is added to briefly describe the effect of vegetation cover on fluvial and hillslope erosion in our model.

In response to RC2 and RC3, we thoroughly revised the methods section in our manuscript, especially the parameter correlation in old Fig. 2, which was previously confusing for the readers. The revisions for RC2 and RC3 were mostly focused in the Methods section (section 3) regarding the applicability and limitations of the datasets used in this study as model input parameters (e.g., NDVI, precipitation, evapotranspiration, etc.).

We have provided the details of manuscript revision in the point-by-point response to the referees' comments. We deeply appreciate your and all referees' efforts to help us improve our manuscript.

The submission file consists of our cover letter, followed by point-by-point response to referees' comments, and the revised manuscript (with tracked-changes) specifying all the modifications made in accordance with the referees' comments.

Please contact us if further clarifications are required.

Sincerely,

Hemanti Sharma and Todd Ehlers (corresponding author).

## **Response to review AR1**

The reviewer's comments are mentioned in black and authors' responses are in blue.

We thank the reviewer for her/his time and efforts in highlighting parts of the manuscript that require changes and clarification.

This paper uses landscape evolution modeling to investigate the relative influence of seasonal precipitation and vegetation variations on erosion rates across four unique climates. The authors drive their LEM with precipitation data and NDVI-derived vegetation cover to determine, across climates ranging from arid to humid temperate, that precipitation outcompetes vegetation cover as a control on erosion, and that these effects vary significantly across the type of climate. Vegetation effects seem to matter most in middle-moisture climates and least in very arid or very humid climates.

The paper deals with an important issue (influence of vegetation on erosion and how we might separate it from precipitation effects). The study design is simple—this is a good thing—and the well-understood suite of study sites provides a nice starting point for the analysis. I do think though that there is one fairly significant (but fixable!) structural weakness in the analysis, and I see a variety of smaller (also fixable) issues related to the treatment and presentation of data and its derived statistics. I could see this paper ultimately being publishable in ESurf, but it will require substantial revision. Below I detail my main concerns and then move on to smaller line comments.

### **Main points:**

1. I feel that the major flaw in this study is the lack of consideration for time lags and intrinsic time scales (in both models and nature). When sediment is eroded from a particular spot in one of these basins, it takes some amount of time to leave the model domain and therefore register as "eroded," rather than just aggrading somewhere other than where it started. We have no real reason to expect that this timescale is less than three months (one season). In fact, field studies often show very long time lags between initial erosion of sediment and its ultimate export from a basin (in addition to further complexity like heavy-tailed distributions of travel times). It is therefore not clear to me why a precipitation or vegetation value for a given season should be plotted against the erosion that occurred during that three-month period (e.g. Figure 5 and others). The authors could certainly evaluate this time lag with initial tests of the model, and/or potentially with data from these catchments if it exists, but at the moment there is a fairly restrictive implicit assumption that these catchments export all eroded sediment within three months. At an absolute minimum the paper should have a subsection in the discussion making this clear and discussing any steps the authors have taken to look at these potential time lags and their effects on the results/interpretations. What would make the paper much more publishable is to run some tests to see how long a pulse of sediment derived from say, one very wet season, takes to leave the catchment.

We agree with the reviewer, that there should be time lags between sediment erosion and its leaving the catchment in the physical sense. However, in this study we only focus on the erosion

when a sediment is removed from its source and plot the same in the results and do not consider the time-lags, which may impact our results and interpretations to some extent.

To capture these time-lags, we ran some tests in the model and compared the precipitation and erosion rate with the concentration of sediment (sediment flux divided by discharge rates) leaving the catchment outlet at a given time-steps for the catchments in Mediterranean and humid settings. We observed a distribution in the concentration of sediment leaving the catchment after a wet season and the time-lags ranged between 3 to 4 seasons in the Mediterranean setting and 1-3 seasons in a humid setting. We have added a subsection (section 5.3, lines 469-490) in the Discussion section in the revised manuscript to discuss this issue and also revisited in the Limitations section (section 5.5, lines 543-549).

2. Aside from Figure 10, all of the prior figures deal with absolute erosion rates relative to absolute values for rainfall/veg cover. But if we are really concerned about system sensitivity, we should care more about proportional changes in forcing and proportional responses. It feels intuitive that a 10 mm/season change in precip might matter more to an arid landscape (in terms of proportional erosion rate change) than a 100 mm/season change in precip matters to a humid-temperate one. I think the authors could give more insight into the responses of the different watersheds if they also used some sensitivity metrics that evaluate proportional forcing and response, not just absolute forcing and response. Figures 4-9 could benefit from extra panels using such metrics.

We agree to the comment and understand that the current representation of data in the figures needs to be modified to account for the system's sensitivity.

To tackle this problem, we have changed Figures 5, 7, and 9 (added 1 more figure, now Fig. 10) to show the relationship between proportional changes (normalized) in forcing (i.e., vegetation cover and/or precipitation rates) and response (erosion rates), with a separate panel for each study area. The plots include information on confidence intervals and correlation coefficients suitable for such scarce data points. In this case, we have used Kendall tau correlation coefficients (which do not require large datasets and do not assume specific distribution of the data). We have also included an extra panel in the above figures to plot the sensitivity coefficients based on the relative change in forcing and response in each setting. The sensitivity coefficients are estimated based on the slope and intercept obtained from regression analysis. These coefficients are only plotted for the study areas where a correlation is obtained between forcing and response with >95% level of significance. For example, in the scenario with constant precipitation and variable vegetation cover (scenario 1), sensitivity coefficients of arid and semi-arid settings are not plotted, as a significant correlation was not observed between the changes in vegetation cover and erosion rates.

3. Methods: I don't think it is sufficient to cite out the key components of the numerical model dealing with how vegetation influences erosion given that this is the entire point of the paper. I know they have been published before, but I ask the authors to please consider presenting them in brief again. Maybe an appendix would be a good place for them?

As per the suggestion of the reviewer, we have added a section in the appendix describing briefly the vegetation influence on fluvial and hillslope erosion in our landscape evolution model, in Appendix (section B) in lines 613-668 in the revised manuscript.

4. In general, figure construction could be much-improved in that the figures could have provided more useful information and been made a lot easier to read. There are issues with overlapping data that could have been made partially transparent, certain data series (the arid landscape data) that really should be shown on a zoomed-in inset because their range of variability is so low relative to others, etc. For all figures, there are serious issues with readability for people with color vision impairments. It is extremely simple to remedy this by using different symbols, line styles, or just color selections that are friendly to all (see colorbrewer or similar tools online). There are a lot of people out there with color vision impairment, and they will have no idea what you're trying to say unless you modify figures 2, 4, 5, 6, 7, 8, 9, and possibly 11.

We agree with the reviewer's comment about the need for improvement in the figure construction. Hence, we have edited Figures 2, 4, 5, 6, 7, 8, 9 and 11 (now Fig. 12) and used different symbols and colours. The problem of the range of visibility for arid datasets has been resolved with the inclusion of separate panels for each study area in Fig. 5, 7, and 9.

5. The statistical treatments presented could also use improvement. Why are we assuming that we are interrogating linear relationships? Do we have theory or data that says all of the relationships examined in this study should be linear? Why do we not see confidence intervals presented to add richness to our interpretations beyond the p-values and correlation coefficients? The statistics here feel like they were done *pro forma* rather than with thought as to the questions being asked and how the stats might or might not contribute to answering them. Yes, the slopes of these linear fits are convenient proxies for model sensitivity to a particular independent variable, but there are many other metrics for sensitivity that don't require assuming this one particular relationship between the variables.

We thank the reviewer for raising an important concern regarding the linearity of the relations presented in the output. To address this issue, we have modified the Figure 2 to exclude the linear regression amongst the model parameters (e.g., precipitation, vegetation cover and ET). However, when we look at the plots with proportional changes in forcing (precipitation and (or) vegetation cover) to the changes in response (erosion rates), we perform linear regression only where the linear relationships are observed (e.g., Figs. 5, 7, 9 and 10) in the revised manuscript. Also, as we are only interested in exploring the sensitivity of one parameter variable at a time (precipitation (P) or vegetation cover (V)), we still rely on the slopes of these linear fits. Also, we have switched from using Pearson correlation coefficient to Kendall tau correlation, which do not require a linear relationship in the variable and also works with scarce data points (as in the case of arid and semi-arid settings). We have also added confidence intervals in Figs. 5, 7, 9 and 10 to add richness to the interpretations.

6. Code/data availability: It feels problematic that the authors have used open-source software that was given DOIs and made available to the community through the efforts of others, and then not

made their own code/data permanently and publicly available. Please help build a community where we archive and share code and data freely by depositing the code, etc that supports this paper in a DOI-stamped repository. I would be surprised if this code/data availability statement is not violating journal policies, funder policies, or both.

We agree with the reviewer about the code/data availability in a DOI-stamped repository. Our version of Landlab and the run-time scripts we used are on GitHub now (for several months). However, as GitHub does not comply with FAIR scientific practices (or provide a DOI), we have created a separate Zenodo entry (with a DOI). We have now included the DOI for this in the “code and data availability” section (line 670) in the revised manuscript. This DOI includes our run-time scripts for all our model simulations, and the input files we used. As we did not directly modify the Landlab or SPACE source code, we will not include that in our submission as it’s already freely downloadable and it only creates confusion to have a duplicate repository on the web.

#### **Line comments:**

Abstract: the last sentence has a low end of 5%, but just above it says 6.5%. Are these different quantities being reported?

The issue has been fixed in the revised manuscript (in line 20) in the revised manuscript.

34: changes play a crucial role. Also the grammar here is odd because seasonality is a noun. Maybe just seasonal?

Thanks for pointing this out. The word ‘plays’ modified to ‘play’ in line 36 and ‘Seasonality’ modified to ‘Seasonal’ in line 35 in the revised manuscript.

39: Or in this case, “plantscape evolution modeling” !!! (just a joke)

We prefer to stick to ‘landscape evolution modeling’ in line 40 in the revised manuscript.

45: If this paper is worth mentioning, you should state its main conclusion rather than just its topic.

The citation is removed from the text from line 45 in the revised manuscript. The paper was not found relevant to the current study.

47: pluralization mismatch—proofread for clarity

Thanks for pointing this out. ‘Decreases’ modified to ‘decreased’ in line 47 in the revised manuscript.

53: do you mean a reduction in sensitivity of soil loss potential to storm frequency?

Yes. Modified in line 53 in the revised manuscript.

54: again here a very vague statement about what past workers did. If it’s worth mentioning, surely it has some relevant conclusion. Also consider restructuring the sentence because differences in vegetation don’t drive erosion and sedimentation.

Thanks for pointing out. Modified in lines 54-55 in the revised manuscript.

56: unclosed (

Modified in line 57 in the revised manuscript.

65: could you state the direction of this effect? I can assume, but haven't read the paper

The increase in vegetation inhibited the effect of runoff (which was temporally constant) resulted in the reduction in sediment yield. The sentence is modified in line 65-67 in the revised manuscript.

66: is this species richness or some other metric?

Thanks for pointing this out. Yes, this is species richness. Modified in line 67 in the revised manuscript.

71-72: "...seasonality in precipitation and vegetation cover conspire to influence..."

Modified in lines 72-73 in the revised manuscript.

74: I suppose it could work either way, but I would have reached for "transience" rather than "transients"

Modified from 'transients' to 'transience' in line 75 in the revised manuscript.

75: "across the extreme..." or "spanning the extreme..."

Modified from 'across' to 'spanning' in line 76 in the revised manuscript.

77: hypothesis 1 sounds strangely tautological. Why not just say "1) P is the first-order driver of seasonal erosion rates." That implies that everything else is of low significance.

Hypothesis 1 shortened in line 78 in the revised manuscript.

121-122: This is fine, but it might be worth adding one sentence to emphasize the limitations of NDVI, chiefly that it saturates out once the ground is basically shrub-covered and so it couldn't tell you much about different plant communities for associated erosion-relevant properties like rooting depth, etc.

A sentence on limitations of NDVI to vegetation cover fraction has been added in lines 128 – 129 in the revised manuscript.

133: Landlab I think(?) is typically written with only "Land" capitalized

Modified from 'LandLab' to 'Landlab' in line 139 in the revised manuscript.

136: typo /

Typo removed in line 149 in the revised manuscript.

137: is this total relief in the whole catchment? Just want to be clear.

Yes. Modified in line 151 in the revised manuscript.

140-143: True, but this is not the only reason you could have initial transience. LEMs (and the systems they represent) have inherent timescales, and you can't know a priori whether the state of the system as captured by the SRTM DEM and your various other inputs is at a full equilibrium condition. Surely it is less likely to be in equilibrium with respect to all relevant forcings than to be in some stage of transient response.

Thanks for the addition. Argument added in lines 156-160 in the revised manuscript.

151: “summing up” can just be “summing”

Modified in line 167 in the revised manuscript.

157: yes and this is fine, but again there are lots of erosion-relevant properties of vegetation that NDVI is NOT good at measuring. It would be good to be up front about this in the writing.

Limitations of NDVI added in lines 176-179 in the revised manuscript.

160: could you provide a few words on the resampling method?

Added in the revised manuscript in line 181.

Figure 2: I wonder about the utility of plotting these things against each other given that we surely expect lags between the water balance and the vegetation response? 182-193 accurately describes the figures, but does not lead us to any real insights about the system. What do you want readers to take away from this figure? Some other points about this figure: Please check that these color schemes are friendly to all (i.e. are color-impaired friendly). I doubt they are, given the use of red and green. An easy remedy would be to use varying marker styles (squares, triangles, stars) in addition to colors. Also panel c would be better if the markers had some transparency so the blue didn't hide the red and the red didn't hide the black. Separate issue: it is not clear to me why we would necessarily expect these relationships to be linear and therefore why one should use a linear regression here to assess correlation. Finally, why don't you label the different data series by their climate rather than by the study area names? Any given reader will only care about the former.

We understand the reviewer's concern about the confusion this figure creates considering the lags between the water balance and the vegetation response. Hence, Figure 2 is now replaced with vegetation and ET relationship and the Budyko curve to capture the aridity and humidity of the systems based on precipitation and evapotranspiration. This would produce more insights in the readers about the systems. Also, in the new figures, we have labelled the datasets based on the climate rather than the study area names, to be clear.

215: This description is, to the extent that I understand these things, not quite right: Landlab is a modeling toolkit, not a model in and of itself (I think of it as a toolbox holding many models, each of which is a possible tool to use). SPACE is one of many *models* that operate within the landlab toolkit or framework.

We thank the reviewer for pointing this out. The lines 241-242 are modified as per the reviewer's comment in the revised manuscript.

222: Was there actually model calibration in the true sense? My read is that you chose values that are appropriate for the study basins, which is 100% fine, but is not the same thing as running an actual calibration exercise.

We thank the reviewer for pointing this out. 'Calibrated' is modified to 'selected for' in line 249 in the revised manuscript.

222-223: Revise this sentence for grammar

Revised line 249-250 for grammar in the revised manuscript.

223: does “erosion” mean erodibility? Save for diffusion/diffusivity. Also lithology is not a model parameter; there are parameters that incorporate the effects of lithology. But these have specific and more descriptive names that we should use.

We thank the reviewer for pointing this out. ‘Erosion’ and ‘diffusion’ have been modified to ‘erodibility’ and ‘diffusivity’ and ‘lithology, tectonic’ have been removed in line 250 in the revised manuscript.

229-230: re-read this sentence for grammatical consistency

Modified lines 256-258 for grammatical consistency in the revised manuscript.

242-243: delete “initial.” It’s just the uplift rate for the whole simulation, which is fine.

Deleted ‘initial’ in line 270 in the revised manuscript.

277: I guess it’s ok if you want to keep it, but I think the units of veg cover are pretty clear so I don’t know how important it is to write [-] after every use. It’s common colloquially to just speak of proportions with no units.

The [-] after every reported vegetation cover fractions have been removed in the revised manuscript.

Figure 4: Modify for color vision impairment viewing; this will be very simple.

Modified the Figure 4 for color vision impairment in the revised manuscript.

Figure 5: same as figure 4. Also the arid data should really be shown on a zoomed-in inset or sub-panel. Just because the arid landscape doesn’t show the same *absolute* response does not mean that it can’t have equal or greater proportional sensitivity than another climate. We can’t evaluate much about this because the black dots are all jammed together in the corner.

We thank the reviewer for pointing this out. Modified the Figure 5 to include separate panels for all climate settings and also a sub-panel for model sensitivity to the proportional changes in the forcing and response.

Figures 6 and 7: same comments about figure readability and construction as 4 and 5.

Modified the Figures 6 and 7 similar to 4 and 5.

Figures 8 and 9: same concerns as above

Modified the Figures 6 and 7 similar to 4 and 5.

Figure 10: Why is this rendered as a line graph? These data are not connected in any sort of sequential relationship (except to the extent that precip varies, but if you wanted to plot that you’d put precip on the x-axis). A bar graph would be better, or a stacked bar graph such that all three plots could be condensed into one. Again here I recommend not using site names but their climate labels.

We thank the reviewer for pointing this out. We have modified the Fig. 10, now Fig. 11 in the revised manuscript, to include a stacked bar graph, where the interpretations from all three scenarios are

condensed into one plot. Also, we have switched from using the names of the study areas to the climate settings.

392-394: Not the best example of agreement with your findings. Rainfall intensity in a plot experiment is not the same as total seasonal precip, so this is a bit of a stretch to use as a direct parallel. The others cited here make sense though.

We agree to the reviewer on using the citation here does not make much sense. Hence, this citation is removed from the text from line 435 in the revised manuscript.

Figure 11: You're probably sick of hearing it, but please just use different markers or line styles or something to distinguish these series.

We have modified the Figure 11 (now Fig. 12) in the revised manuscript by using different markers for color vision impairment.

442-443: This sentence is vague. How do the dynamics change as a result of changes in veg?

We thank the reviewer for pointing this out. The sentence has been modified to "significant changes in landscape pattern and vegetation coverage (i.e., land use land cover) might contribute to long-term dynamics of soil loss", for clarity in lines 506-507 in the revised manuscript.

471: "subject to"

Modified in line 534 in the revised manuscript.

486: All of these limitations are fine, but the biggest limitation of the study is that there is no mechanism to consider transient dynamics, for example that sediment eroded off a hillslope in March might take until December to move out of the model domain.

We thank the reviewer for pointing this out. We have added this argument in the model limitations in lines 541-547 in the revised manuscript.

642: see main point above.

The model code and data is registered to a DOI-stamped repository (i.e., Zenodo) and is now mentioned in the "code and data availability section" in line 670.

## **Response to review AR2**

The reviewer's comments are mentioned in black and the authors' responses are in blue.

We thank the reviewer for her/his time and efforts in highlighting parts of the manuscript that require changes and clarification.

This paper investigates a fundamental question-- sensitivity to of erosion to climate across a large eco-climatic and geomorphic gradient. This problem is especially hard to address over long time scales where topography reflect the long term meory of the regional climate. The auuthors should be commented for tackling such a difficult problem. The paper can be reconsidered after major revisisons.

**Regional geomorphic context:** More information is needed on geomorphology and the erosion history of the study sites. How different are geomorphologies of these different sites. A slope-area plot for each catchment would be telling. Are there landslides or dry soil/rock slides in these watersheds. What is the erosional history of this region, is the landscape in steady-state or dynamic equilibrium with uplift and climate. What periods do the modern uplift rates cover? Do the millennial erosion rates bracket the uplift rates. Ideally, in order to study the role of climate on erosion rates wouldn't you need to calibrate your model for each site to targeted erosion rates. That means that in every site your erodibility etc parameter would need to vary in relation to your topography. The key is that, as the authors would appreciate, the ecoclimatic and tectonic legacy of the system is engraved in the soil/erodibility and topographic properties, if you use the topo from today then you will need to do a calibration to the rest of the parameter space of your model. At least that is my opinion, but I appreciate a justification. Also the "detrending" concept is not well explained in the paper, actually what the authors did was not presented.

We agree with the reviewer that calibration of our model to geomorphic and topographic properties for each study site would result in more accuracy in the output. Unfortunately, the observations required for this are not available. In addition, it is nearly impossible for a landscape evolution model to reproduce reality due to uncertainties in the initial topography, and many material properties. Conversely, a 'purely modelling' approach on synthetic topographies without a connection to reality is never satisfying because readers are left wondering how it relates to reality. The philosophy behind this study, and our previous work, is to present a sensitivity analysis to an assumed set of physics to different forcings. In our case, we do this for the effects of changing precipitation (P) and/or vegetation cover (V) on catchment erosion at a seasonal timescale, we keep all other parameters (e.g., uplift rates, erodibility, etc.) constant. The text (end of the introduction, lines 88-92) has been modified to reflect this better and state that we present a series of sensitivity analyses 'tuned' to reality for different ecological settings. These sensitivity analyses are data-driven with observed precipitation and vegetation cover histories, but are by no means intended to accurately reflect all aspects of reality of the catchments studied due to large uncertainties in material properties and forcing conditions (e.g., rock uplift rates). In addition, the text already mentioned similar limitations (lines 548-555). Given our approach of conducting a sensitivity analysis tuned to reality, we think it unnecessary to provide additional details

for each study area here, that are already summarized in other studies we cite (Bernhard et al., 2018; Oeser et al., 2018; Schaller et al., 2018).

Finally, we highlight that another reason to use modern topography is to incorporate the spatial distribution of vegetation cover (in the form of NDVI). The landscape is not in a steady state but in dynamic equilibrium with uplift and climate. The uplift rates used in this study are not the absolute values, but the best-fit estimates based on the literature (van Dongen et al., 2019) and our previous modelling study at millennial timescales (Sharma et al., 2021).

The detrending is performed to remove the effects of long-term transients introduced in the model output due to the differences in model parameters and actual forcings leading to the evolution of the topography in the regions of interest. To avoid the effects of these long-term transience (mostly due to rock uplift rates), we performed linear detrending. The detrending was conducted through a linear regression over entire time series of 1000 years and the values were corrected using the slope of the regression line. This explanation is modified in the main text in the revised manuscript in lines 291-293.

**Climate forcing:** how can you simulate this model at seasonal time steps (lines 224-225), especially in arid and semiarid climates, where the only way to get erosive runoff would be to capture high-intensity storms. Your seasonal rainfall model will not capture the role of extreme events. Furthermore, how do you solve equation 1 to obtain runoff in seasonal time scales. How do monthly simulations even give you runoff in the drier sites. I know ET and P are inputs, but the infiltration equation won't produce any runoff unless you have intense storms-- a seasonal time step would only produce drizzles. Am I missing a detail somewhere?

The reviewer raises an important point about how the stochasticity of precipitation and extreme events could create additional complications when interpreting our results. We agree with the reviewer that this could be an issue and the effects of extreme events on catchment erosion in these study areas is in fact the topic of a separate paper we have prepared (and the final chapter in H. Sharma's PhD dissertation). We were initially hoping to consider shorter timescales (relative to extreme events) in this manuscript, but the results ended up being too complicated and also long to be considered. More specifically, we found that an adequate analysis of extreme events requires a substantial amount of additional figures and text and we wouldn't be able to give a balanced discussion of it within this manuscript. The model setup also had to be different. Given this, we chose to focus on seasonal averages here. However, to accommodate the reviewer's concern and inform readers of potential caveats associated with this, we have added a paragraph of text in the methods section (line 139-143 in revised manuscript) stating this study focuses on average changes in erosion rates that occur over seasonal time scales. In addition, we clearly state that extreme events (e.g. from El Nino) are not considered, and these effects would be superimposed upon what we present here. We provide some information based on the frequency of known extreme events in the region (beyond the 20 years we consider) as well as how these effects are most pronounced in the north, and less so in the southern study areas. Finally, for the reviewers benefit we note here that the direction and type of response that

occurs during extreme events is not inconsistent with the results presented here – although given that the magnitude of extreme events (El Nino) decreases from north to south in our study areas (i.e., it's more pronounced in N. Chile) and it requires significant explanation to present.

In addition, how can we assure that this 20 years of observed weather properly captures the statistical properties of the regional climate. A better approach would be to train a stochastic weather generator and run it for 1000 years without cycling the same rainfall.

To address this concern, we clearly state when the statistics are reported that these are for the mean seasonal behaviour of changes in erosion, and do not account for extreme events, which would be superimposed upon the effects described here (depending on the season when they occur). We also note for the reviewer that their suggestion of using a stochastic weather generator would be counter to the entire approach of the paper which is to use observed records of climate and vegetation. If a stochastic weather generator was used then we wouldn't be able to run the simulations with an observed vegetation cover for each season. We also note that meteorological records >10 years are typically considered to capture the climate of a region (although don't necessarily capture extreme events). In fact, in the climatology and climate modelling communities, 10 years of data are typically used for climate characterization. In our case, we use a 20-year record. If a 1000-year stochastic weather generator was used we would have no way to calibrate the return time, magnitude, and duration of events and it would shift the entire approach of the study away from being observationally driven to being a pure modeling study.

Equation (1), please explain how water balance was resolved. Normally ET should be resolved in the model with given P, but my sense is that ET is an external input to the model. If that is so, then P should be used from the same data set. I think reanalysis is a model product, so you need to be consistent because in dry landscapes you may end up with a greater ET than P because of data set differences. Also why not use runoff from reanalysis too if ET is from reanalysis.

We agree with the reviewer that ideally ET should be resolved within the model with the given P. And the inconsistency of P and ET would result in problems in dry landscapes. To address the above concern the minimum value of P and ET was used for ET. We have added this argument in the revised manuscript in lines 224-226.

Secondly, for the calculation of ET (e.g., using the Penman-Monteith equation) additional parameters are required such as solar radiation, temperature, wind speed, humidity, crop factor etc. Although we have weather station observations of the above parameters for the last 4 years (i.e., 2016-2020) (Übernickel et al., 2020), we did not extrapolate the data for the whole time series, as we use precipitation and vegetation cover (NDVI) observations. We preferred to use the ET as input to avoid any stochastic effects in the ET (as we use actual precipitation distribution) to be consistent to the best of our capacity.

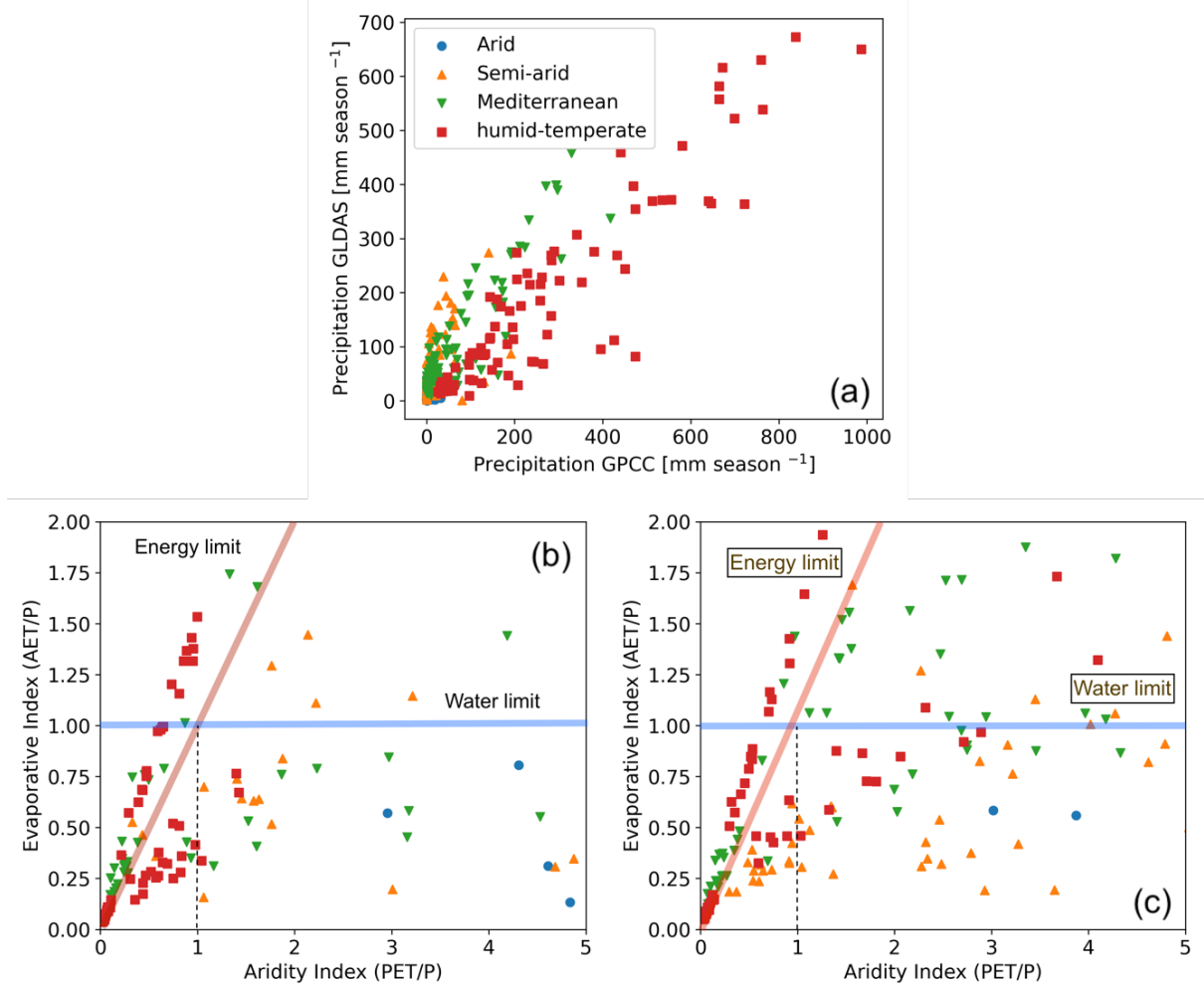


Figure 1. Relation between the water balance datasets obtained from GPCC and GLDAS NOAH reanalysis products with (a) seasonal precipitation rates obtained from GPCC and GLDAS NOAH, (b) Budyko curve for precipitation data from GPCC and ET (and PET) from GLDAS NOAH, and (c) Budyko curve for both precipitation and ET (and PET) from GLDAS NOAH model.

When we compare the seasonal precipitation rates from GPCC (which is based on ground-based observations) and GLDAS NOAH (which is a reanalysis product). The trend of the data is linear, with slightly lower values obtained from GLDAS NOAH (Fig. 1a). However, if we compare the Budyko curves used in our study (Fig. 1b) and with ET and P both from GLDAS NOAH (Fig. 1c), we observe a similar pattern in aridity and evaporative index in humid setting, but lesser ET than P in most of the seasons in other climates. Hence, we preferred using the P dataset from ground-based observations and not from the same dataset from where ET and PET were extracted.

We did not use the runoff from reanalysis because we preferred to estimate the soil water infiltration in our model based on the soil properties (bulk density, soil moisture, porosity, etc.) specific to the study sites.

**Vegetation input in models:** Figure 2a was ndvi data converted veg cover fraction? This was not told in the text. (a) Why is there a generally negative relationship between Seasonal P and fractional veg cover. In the wet site there seems to be two separate data group both of which show slightly negative r. (b) there is so much variability in seasonal ET and veg cover, how is this relationship built in the model? Data from NA shows a strong negative sign between ET and veg cover, how is that possible. I doubt the accuracy of the Reanalysis data, is there an independent way to check this. Similarly, ET-P relationship does not make any sense at the landscape scale. I read the argument for some of these as the steep gradients of temperature, precip, solar radiation, and that make sense, if you introduce the spatial variability vegetation you will need that for hydrology as well as vegetation is variable because of spatial precip and ET etc. That is also true for edibility and threshold related to veg. Does the erosion threshold vary with veg cover.

We thank the reviewer for pointing out a very important concern related to the correlation of model input parameters. In response of the first reviewer's comment regarding the utility of figure, we have modified Figure 2 and removed the subsection with direct relationship of precipitation and vegetation cover. Also, after rechecking the datasets for ET, we realized that we plotted PET (instead of ET) in this figure. We deeply regret the inconvenience caused by us for the reviewers (thanks for helping us find this!). In the revised manuscript we present the relation between vegetation cover and ET, and a Budyko curve using the same datasets. Please find the point wise response to above comment below:

- (a) We expect some time-lags between the water balance and vegetation response. For example, the positive vegetation change owed to a wet season is expected to be observed in the following season, which may be drier than the previous. The above relation led to the negative relationship between seasonal P and fractional veg cover. As Figure 2a did not provide a meaningful insight into the system, hence, it is not presented in the revised manuscript.
- (b) The confusion created due to figure construction (old Fig. 2c) has been corrected in the revised manuscript (now Fig. 2a). In the modified Fig. 2a, we now observe two clusters of data for the study area in humid climate (formerly written as NA). Here, we observe a positive trend in vegetation and ET separately for summer (with veg cover between 0.55 and 0.75) and winter (with veg cover between 0.7 and 0.85). The higher ET ( $150 - 350 \text{ mm season}^{-1}$ ) in summer may be owed to high temperatures in summer (dry season), where soil moisture may also contribute to ET in addition to P. Also, during winter (wet season) ET is relatively lower (i.e.,  $30 - 120 \text{ mm season}^{-1}$ ) for higher veg cover owing to low temperatures. It is also worth noting the vegetation cover does not depend solely on precipitation, and also responds to temperature, and less importantly to seasonal variations in solar radiation.

The ET-P relationship is now plotted using a Budyko curve. The study incorporates spatial variability on vegetation cover, with uniform P and ET. The erodibility varies with vegetation cover. However, erosion threshold does not vary with vegetation cover. The above description is added in lines 204-217 in the revised manuscript.

Figure 2 can be augmented with a Budyko curve using the same data sets. The reason is that, it is hard to imagine to have such large carry over mechanisms of soil moisture in these environments to yield a negative relationship between seasonal P and ET. if carry over is neglected Figure 2 c is not physically possible-- zero precip leads to the highest ET? Am I missing the point?

As per reviewer's suggestion, we have modified the Figure 2 to include the Budyko curve using the same datasets. Earlier, the confusion was created in the Fig 2c with the highest ET at zero precipitation due to an error by the authors. In the revised figure, we observe carry-over mechanisms of soil moisture for a couple of seasons in mostly humid and semi-arid settings in dry seasons following a wet season. This explanation is added in the main text in methods section (lines 204-217).

Fig 5—inverse correlation of erosion with vegetation only makes sense if hillslope diffusion is constant. Given this impressive precip gradient, I suspect hillslope diffusion should also depend on precip. I don't see a variable hillslope diffusion in the model parameters table.

The catchments considered in this study are mainly fluvially dominated and hillslope diffusion is very low in comparison to fluvial erosion (when plotting erosion rates by the individual processes – not shown in the study), mostly in Mediterranean and humid-temperate settings. Also, the diffusion coefficient is also dependent on, and time varying with, the vegetation cover (see section B1 in lines 616-627 in Appendix B in the revised manuscript). We have added lines 315-317 in results section 4.1 in the revised manuscript, to emphasize on the above point.

van Dongen, R., Scherler, D., Wittmann, H., and von Blanckenburg, F.: Cosmogenic  $^{10}\text{Be}$  in river sediment: where grain size matters and why, *Earth Surf. Dyn.*, 7, 393–410, <https://doi.org/10.5194/esurf-7-393-2019>, 2019.

Sharma, H., Ehlers, T. A., Glotzbach, C., Schmid, M., and Tielbörger, K.: Effect of rock uplift and Milankovitch timescale variations in precipitation and vegetation cover on catchment erosion rates, *Earth Surf. Dyn.*, 9, 1045–1072, <https://doi.org/10.5194/esurf-9-1045-2021>, 2021.

Übernickel, K., Ehlers, T. A., Ershadi, M. R., Paulino, L., Fuentes Espoz, J.-P., Maldonado, A., Osés-Pedraza, R., and von Blanckenburg, F.: Time series of meteorological station data in the EarthShape study areas of in the Coastal Cordillera, Chile, <https://doi.org/10.5880/FIDGEO.2020.043>, 2020.

## **Response to review AR3**

The reviewer's comments are mentioned in black and authors' responses are in blue.

We thank the reviewer for her/his time and efforts in highlighting parts of the manuscript that require changes and clarification.

An interesting paper. Definitely suitable for ESurf. Three simulation scenarios hold the idea of comparing the role of temporal changes of driving and resisting force in sediment production. The climate range of the study sites bring another level of complexity and explanation. These are cool.

I understood the competition between the driving and resistance forces on sediment yield. In the first two scenarios, one of them keeping constant another force is varied. In the third one, both are changing. Arid, semi-arid, wet seasons are relatively easier to comprehend where are in the first and third regions – very low runoff has little impact and no vegetation growth in arid case, or runoff production does not change vegetation more due to (maybe ecosystem shift from water limitation to energy limitation, space competition etc.) (please see fig 12 of Collins and Bras, 2010-WRR) [Similar to Douglas (1976); Fournier (1960); Wilson (1969) can be found in Walling and Kleo (1979)]. However, the beauty of the study in investigating the case of Mediterranean climate when the mismatch between vegetation growth (summer time) and runoff production (winter).

My questions are:

1. Seasonal timestep confused me a bit. How do you relate the erosion rate to vegetation cover directly? Let me clarify. Wet season may cause greater vegetation cover and may also greater erosion rates. Or vice versa. But when erosion rates are greater than the uplift rate slopes are getting gentler. The following wet or dry season, the erosion rates will be relatively less responsive to the vegetation cover and/or runoff production. To summarize my question:

In this kind of long-time steps (seasonal here), the relationship between erosion rate and vegetation cover may be affected by inherited simulated slope (refers to energy in shear stress formula) values from previous season (model time step). So, I am suspicious that the signal may be blended.

We thank the reviewer for raising a very important concern about the direct relation of seasonal vegetation cover and erosion rates. We tried to establish a relation between the seasonal changes in vegetation cover to that of catchment erosion rates in this study but did not consider the effects of inherited slopes from previous season. To address this concern, we have added the above argument in the methods section in the revised manuscript (lines 143-145). Please also see our response to reviewer 2 (above) concerning the consideration of extreme events.

1. One of the sites (Nahuelbuta) has a MAP of 1400 mm. If NDVI is notorious for saturation problem (fig. 16 from Huete et al., 2002 - RemSenEnv), NDVI to vegetation cover conversion maybe affected from this problem. You mentioned NDVI values reach up to 0.8. So, in shear stress partitioning (most probably you are using it based on nv, ns etc. from your Table 1) maybe affected from the NDVI to vegetation cover fraction conversion.

We thank the reviewer for raising a very important concern about the effect on shear stress partitioning due to the saturation problem in NDVI in the high biomass region i.e., in the humid temperate setting. To address this concern, we have added the above argument/caveat you mention in the methods section in the revised manuscript (lines 176-179). We don't really have a way to get around this problem as there are no other data sets for these diverse study areas with a suitable time series of vegetation change.

Need clarification:

1. In Figs 5, 7, and 9: There should be 20 filled and 20 hollow circles for each site. Is not it? When I try to count, I counted more than 20 or less. Less may be understandable due to overlap. But why more? Did I miss something there?

The reviewer raised a very important point here about the number of points representing wet and dry seasons in the figures. In our study, we have divided all the seasons in a year into either wet or dry, to capture the erosion at any time of the year (see Table 1). So, in this case, if erosion occurs in all the four seasons in a year, there may be a maximum of 40 filled and/or hollow dots in the Figs. 5, 7, and 9 in the unrevised manuscript.

However, in the revised manuscript, we have modified our approach in plotting the changes in forcing and response (by switching to plot the normalized changes in Figs. 5, 7, 9 and 10 in revised manuscript), irrespective of wet or dry seasons to minimize the confusion. We did this to effectively focus on the main question asked in this study.

I have following minor edits:

L71. ...the seasonality in precipitation and vegetation covers ARE.... 'is' or 'are'?

The sentence is modified in the revised manuscript and 'are' is removed because of grammatical inconsistency.

L92. Santa Gracia National Reserve.. Upper case for National Reserve.

Modified from lower 'nature reserve' to 'Nature Reserve' in line 96 in the revised manuscript.

L98-9. Use lower case for compass directions. ...in the north... ...in the south... L94.

Modified from upper case to lower case for compass directions in lines 98-99 and 103-104 in the revised manuscript.

L103. Comma after 'respectively'.

Modified in line 108 in the revised manuscript.

L107. Capitalize 'plate'. ...the Nazca Plate ... ...the South American Plate....

Modified in line 112 in the revised manuscript.

L128. Comma after '(section 3.5)'.

Added comma after '(section 3.5)' in line 134 in the revised manuscript.

L136. Typo. Delete '/'.

Deleted typo '/' in line 149 in the revised manuscript.

L139. Word order. Either 'Considered catchment sizes'... or 'Investigated catchment sizes'....

Modified from 'Considered catchment sizes'... to 'Investigated catchment sizes in line 152 in the revised manuscript'.

L140. Insert comma after 'La Campana'.

Modified in line 153 in the revised manuscript.

L145. It may be better to include/mention that the spatial resolution is ~111 km at the equator. At your study sites (26°S to 38°S), it is shorter than this value.

As this is the point data, mentioning the spatial resolution as 1 degree would be sufficient. Mentioning the resolution in km would create confusion. Hence, it is removed the text in line 162 in the revised manuscript.

L149. Do not capitalize seasons. Also L225.

Modified in lines 166 and 252 in the revised manuscript.

L149. Do not capitalize 'austral'.

Modified in line 166 in the revised manuscript.

L150. Word choice. 'Illustrated' or 'given'. Please reconsider.

Modified from 'Illustrated' to 'given' in line 167 in the revised manuscript.

L319. Comma after '(LC)'.

The text has been modified in the revised manuscript, and no longer include the manuscript.

L319. It may be better '(Figs. 6 and 7)' ...

The text has been modified in the revised manuscript, and no longer include the manuscript.

L532. If the given 'porosity' parameter (0.20) for loam soil, it is a bit lower than the reported values in the literature.

We thank the reviewer for pointing out this typo. This value belongs to our previous publication and not used in this study. In this study we use different porosities estimated from the bulk density of the soil types for each study area (as mentioned in Table A1 in Appendix A in line 610 in the revised manuscript).

We use different porosities

- a) You cited Istanbulluoglu and Bras (2006) for infiltration values in Eq.3. However, table 1 of Istanbulluoglu and Bras (2006) used porosity as 0.45 for loam. Moreover, in table 2 of Clapp and Hornberger (1978), they gave 0.451 (0.078) (std dev.) for loam, 0.420 for sandy clay loam.

We estimated the porosities in each study area based on reported values of bulk densities in the study areas citing Bernhard et al., (2018) in Table A1 in Appendix (line 611 in revised manuscript). The estimated porosities range from 0.43-0.51 in sandy loam to 0.7 in sandy clay loam.

- b) When, I read L170-174, bulk densities vary from  $800 \text{ kg m}^{-3}$  to  $1500 \text{ kg m}^{-3}$ . Let's assume the density of quartz is  $2650 \text{ kg m}^{-3}$ . Your density should vary from  $\sim 0.43$  to  $\sim 0.70$ . Please check.

I assume the reviewer meant 'porosity' in this comment. Please refer the response to previous comment.

1 **Effects of seasonal variations in vegetation and precipitation on  
2 catchment erosion rates along a climate and ecological gradient:  
3 Insights from numerical modelling**

4 Hemanti Sharma<sup>1</sup> and Todd A. Ehlers<sup>1,2</sup>

5 <sup>1</sup>Department of Geosciences, University of Tübingen, Schnarrenbergstr. 94-96, 72076, Germany

6 <sup>2</sup>School of Geographical and Earth Sciences, University of Glasgow, Glasgow, Scotland

7 Correspondence to: Todd A. Ehlers (todd.ehlers@uni-tuebingen.de)

8 **Abstract.** Precipitation in wet seasons influences catchment erosion and contributes to annual erosion rates. However, wet  
9 seasons are also associated with increased vegetation cover, which helps resist erosion. This study investigates the effect of  
10 present-day seasonal variations in rainfall and vegetation cover on erosion rates for four catchments along the extreme climate  
11 and ecological gradient (from arid to temperate) of the Chilean Coastal Cordillera ( $\sim 26^{\circ}\text{S}$  –  $\sim 38^{\circ}\text{S}$ ). We do this using the  
12 Landlab-SPACE landscape evolution model, ~~using a set of runtime scripts and input files~~, to account for vegetation-dependent  
13 hillslope-fluvial processes and hillslope hydrology. Model inputs include present-day (90 m) topography, and a timeseries  
14 (from 2000–2019) of MODIS-derived NDVI for vegetation seasonality; weather station observations of precipitation; and  
15 evapotranspiration obtained from GLDAS NOAH. Simulations were conducted with a step-wise increase in complexity to  
16 quantify the sensitivity of catchment scale erosion rates to seasonal ~~average~~ variations in precipitation and/or vegetation cover.  
17 Simulations were conducted for 1,000 years (20 years of vegetation and precipitation observations repeated 50 times). After  
18 detrending the results for long-term transient changes, the last 20 years were analyzed. Results indicate that when vegetation  
19 cover is ~~variable~~ but precipitation is held constant, the amplitude of change in erosion rates relative to mean erosion rates  
20 ranges between 5% (arid) to 36% (Mediterranean setting). In contrast, in simulations with variable precipitation change and  
21 constant vegetation cover, the amplitude of change in erosion rates is higher and ranges between 13% (arid) to 91%  
22 (Mediterranean setting). Finally, simulations with coupled precipitation and vegetation cover variations demonstrate variations  
23 in catchment erosion of 13% (arid) to 97% (Mediterranean setting). Taken together, we find that precipitation variations more  
24 strongly influence seasonal variations in erosion rates. However, the effects of seasonal variations in vegetation cover on  
25 erosion are also significant (between 5–36%) and are most pronounced in semi-arid to Mediterranean settings and least  
26 prevalent in arid and humid-temperature settings.

**Deleted:** modified

**Formatted**

**Deleted:** varied

**Deleted:** 6.

**Deleted:** humid-temperate

27 **Keywords:** Landlab, vegetation, Chilean Coastal Cordillera, biogeomorphology, seasonality, precipitation, [EarthShape](#).

28 **1 Introduction**

29 Catchment erosion rates vary spatially and temporally (e.g., Wang et al., 2021) and depend on topography (slope, Carretier et  
30 al., 2018), vegetation cover and type (e.g., Zhang et al., 2011; Starke et al., 2020; Schaller and Ehlers, 2022) and precipitation  
31 rates (e.g., Cerdà, 1998; Tucker and Bras, 2000). Over annual timescales, temporal variations in catchment erosion occur in  
32 response to seasonal variations in precipitation and vegetation cover. For example, previous work has found that a significant  
33 fraction of annual erosion occurs during wet seasons, with high runoff rates (Hancock and Lowry, 2021; Leyland et al., 2016;  
34 Gao et al., 2021; Wulf et al., 2010). However, this increase in precipitation during wet seasons also promotes vegetation  
35 growth, which in turn influences erosion rates (Langbein and Schumm, 1958; Zheng, 2006; Schmid et al., 2018). ~~Seasonal~~ and  
36 longer-term ~~changes in both precipitation and vegetation cover~~ play a crucial role in intra-annual changes in erosion rates  
37 (Istanbulluoglu and Bras, 2006; Yetemen et al., 2015; Schmid et al., 2018; Sharma et al., 2021). The intensity, frequency, and

**Deleted:** Seasonality,

**Deleted:** ,

**Deleted:** plays

45 seasonality of precipitation and vegetation cover change within a year depend upon the climate and ecological conditions of  
46 the area of interest (Herrmann and Mohr, 2011). One means of investigating the effects of seasonality in precipitation and (or)  
47 vegetation cover on erosion rates is through landscape evolution modeling (LEM), which can be parameterized for variations  
48 in vegetation-dependent hillslope and fluvial processes over seasonal time scales.

49 Previous modeling and observational studies have investigated the effects of seasonality in precipitation and vegetation on  
50 catchment erosion. Bookhagen et al., (2005), Wulf et al., (2010), and Deal et al., (2017) investigated the effects of stochastic  
51 variations in precipitation on erosion and sediment transport in the Himalayas. They found that high variability in rainstorm  
52 days (>80% of MAP) during the wet season (summer monsoon) caused high variability in the suspended sediment load. Similar  
53 seasonality in sediment loads was reported in a field study in Iran, using sediment traps and erosion pins. These authors  
54 concluded that wet seasons experienced maximum erosion rates (>70% of annual), which decreased in dry seasons (<10% of  
55 annual) (Mosaffaei et al., 2015). Field observations in the heavily vegetated Columbian Andes concluded that soil erosion and  
56 nutrient losses are significantly influenced by precipitation seasonality (Suescún et al., 2017). In contrast, work by Steegen et  
57 al., (2000) in a loamy agricultural catchment in central Belgium found suspended sediment concentrations in streams were  
58 lower during summer (wet) rather than winter (dry) months due to the development in vegetation cover in the wet season.  
59 Other workers have found a dependence of seasonal erosion on ecosystem type. For example, Istanbulluoglu et al., (2006)  
60 found a reduction in the sensitivity of soil loss potential to storm frequency in humid ecosystems compared to arid and semi-  
61 arid regions. Work by Wei et al., (2015) in the semi-arid setting of the Chinese Loess Plateau, reported that significant changes  
62 in vegetation related land use/land cover may contribute to long-term soil loss dynamics. However, seasonal variations in  
63 runoff and sediment yield are mainly influenced by intra-annual rainfall variations. Finally, previous work in a Mediterranean  
64 environment by Gabarrón-Galeote et al., (2013) described rainfall intensity as the main factor in determining hydrological  
65 erosive response, regardless of the rainfall depth of an event.  
66 When looking at seasonal vegetation changes in more detail, several different studies suggest these changes are important for  
67 catchment erosion. For example, Garatuza-Payán et al., (2005) emphasized that seasonal patterns in erosion are strongly  
68 influenced by plant phenology as demonstrated by the changes in vegetation cover (measured by NDVI). A similar study on  
69 the Loess Plateau, China, by Zheng (2006) documented decreasing soil erosion as vegetation cover increases during the wet  
70 season. Work conducted in a forested setting (Zhang et al., 2014) documented the importance of tree cover as an effective  
71 filter for decreasing the effects of rainfall intensity on soil structure, runoff, and sediment yield. Numerical modeling studies  
72 have also found a significant impact of vegetation on erosion. For example, Zhang et al., (2019) found that when precipitation  
73 was kept constant, the increase in vegetation cover resulted in a significant reduction in sediment yields (20-30% of the total  
74 flux). Also, during early to mid-wet season, the species richness and evenness of plant cover both play an essential role in  
75 reducing erosion rates during low rainfall events (Hou et al., 2020). However, in the case of high-intensity rainfall events at  
76 the start of a wet season, when vegetation cover is low, the duration and intensity of rainfall were found to significantly affect  
77 erosion rates (Hancock and Lowry, 2015). Other work conducted in a Mediterranean environment points to the coincidence of  
78 peak rainfall erosivity in low vegetation cover settings, leading to an increased risk of soil erosion (Ferreira and Panagopoulos,  
79 2014). Despite potentially conflicting results in the previous studies, what is clear is that seasonality in precipitation and  
80 vegetation cover conspire to influence catchment erosion, although which factor (precipitation or vegetation) plays the  
81 dominant role is unclear.  
82 This study complements the previous work by applying a Landscape Evolution Model (LEM) to investigate seasonal transience  
83 in catchment erosion due to variations in precipitation and vegetation. We do this for four locations spanning the extreme  
84 climate and ecological gradient (i.e., arid, semi-arid, Mediterranean, and humid temperate) in the Chilean Coastal Cordillera.  
85 Our efforts are focused on testing two hypotheses: (1) precipitation is the first-order driver of seasonal erosion rates, and (2)  
86 catchment erosion in arid and semi-arid regions is more sensitive to seasonality in precipitation and vegetation than the

**Deleted:** on

**Field Code Changed**

**Field Code Changed**

**Deleted:** Work by Chakrapani (2005) identifies the control of mean local relief and seasonality in precipitation on sediment load in rivers. Similar seasonality in sediment loads was reported in a field study in Iran, using sediment traps and erosion pins.

**Deleted:** have

**Deleted:** decreases

**Deleted:** the

**Deleted:** season

**Deleted:** documented

**Deleted:** differences

**Deleted:** erosion and sedimentation

**Deleted:** (

**Deleted:** as

**Deleted:** is

**Deleted:** effect of

**Deleted:** change on

**Deleted:** is significant

**Deleted:** the

**Deleted:** the

**Deleted:** covers are co-

**Deleted:** transients

**Deleted:** in

**Deleted:** of

**Deleted:** if

**Deleted:** , then the influence of seasonal changes in vegetation cover would be of low significance

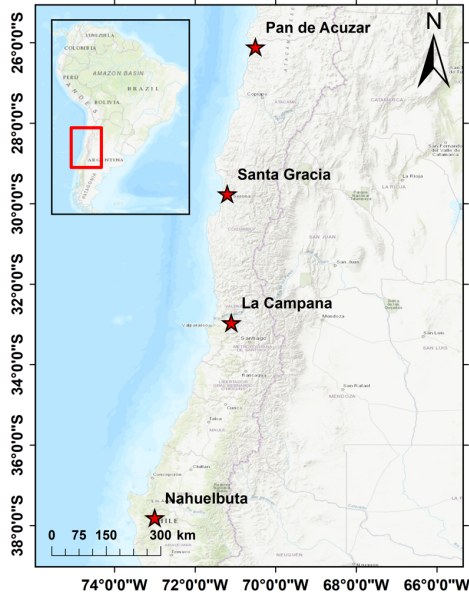
115 Mediterranean and humid temperate regions. To test the above hypotheses, we conduct a sensitivity analysis of fluvial and  
116 hillslope erosion over four Chilean study areas to investigate the individual effects of seasonal changes in vegetation cover  
117 and precipitation compared to simulations with coupled variations in precipitation and vegetation cover. We do this using a  
118 two-dimensional LEM (the Landlab-SPACE software), which explicitly handles bedrock and sediment entrainment and  
119 deposition. We build upon the approach of Sharma et al., (2021) with the additional consideration of soil-water infiltration.  
120 Our model setup ~~broadly representative of the present-day~~ conditions in the Chilean Coastal Cordillera (Fig. 1) and ~~uses~~  
121 ~~present-day inputs such as~~ topography from SRTM DEMs (90 m) for four regions with different climate/ecological settings.  
122 Simulations in these different ecosystems are ~~driven~~ by observed variations ~~in~~ vegetation cover from MODIS NDVI (between  
123 2000 – 2019) and observed precipitation rates over the same time period from neighboring weather stations. ~~We note that the~~  
124 ~~aim of this study is not to reproduce reality in these study areas. This is due to the uncertainties in the LEM initial conditions~~  
125 ~~and material properties, and rock uplift rates. Rather, our focus is a series of sensitivity analyses that are loosely ‘tuned’ to~~  
126 ~~natural conditions and observed vegetation and precipitation changes along an ecological gradient. As shown below, these~~  
127 ~~simplifications facilitate identifying the relative contributions of vegetation and precipitation changes on catchment erosion.~~

**Deleted:** is focused on  
**Deleted:** use as input  
**Deleted:**  
**Deleted:** drive

## 128 2 Study Areas

129 This section summarizes the geologic, climate, and vegetation settings of the four selected catchments (Fig. 1) investigated in  
130 the Chilean Coastal Cordillera. These catchments (from north to south) are located in the Pan de Azúcar National Park (arid,  
131 ~26°S), Santa Gracia ~~Nature Reserve~~ (semi-arid, ~30°S), and the La Campana (~~Mediterranean~~, ~33°S) and Nahuelbuta  
132 (temperate-humid, ~38°S) national parks. Together, these study areas span ~1,300 km distance of the Coastal Cordillera. These  
133 study areas are chosen for their steep climate and ecological gradient from ~~north~~ (arid environment with small ~~to no~~ shrubs) to  
134 ~~south~~ (humid temperate environment with evergreen mixed forests) (Schaller et al., 2020). The study areas are part of the  
135 German-Chilean priority research program EarthShape ([www.earthshape.net](http://www.earthshape.net)) and ongoing research efforts within these  
136 catchments.

**Deleted:** nature preserve  
**Deleted:** mediterranean  
**Deleted:** North  
**Deleted:** South  
**Field Code Changed**



145

146 **Figure 1.** Study areas in the Coastal Chilean Cordillera ranging from an arid environment in the north (Pan de Azúcar),  
 147 semi-arid (Santa Gracia), Mediterranean (La Campana), and humid temperate environment in the south (Nahuelbuta).  
 148 The above map is obtained from the Environmental System Research Institute (ESRI) map server  
 149 ([https://services.arcgisonline.com/ArcGIS/rest/services/World\\_Topo\\_Map/MapServer](https://services.arcgisonline.com/ArcGIS/rest/services/World_Topo_Map/MapServer), last access: 25 April 2022).

150 The bedrock of the four study areas is composed of granitoid rocks, including granites, granodiorites, and tonalites in Pan de  
 151 Azúcar, La Campana, and Nahuelbuta, respectively, and gabbro and diorites in Santa Gracia (Oeser et al., 2018). The soil  
 152 types in each catchment were identified as a sandy loam in three northern catchments (with high bulk density: 1300 – 1500 kg  
 153 m<sup>-3</sup>) and sandy clay loam in Nahuelbuta (with lower bulk density: 800 kg m<sup>-3</sup>) (Bernhard et al., 2018). The western margin of  
 154 Chile along the latitudes of the different study areas is characterized by a similar tectonic setting whereby an oceanic plate  
 155 (currently the Nazca Plate) has been subducting under the South American Plate since the Palaeozoic. Despite this common  
 156 tectonic setting along, slight differences in modern rock uplift rates are documented in the regions surrounding the three  
 157 northern catchments (i.e., < 0.1 mm yr<sup>-1</sup> for ~26 °S to ~33 °S) (Melnick, 2016) and the southern catchment (i.e., 0.04 to > 0.2  
 158 mm yr<sup>-1</sup> for ~38 °S over the last 4±1.2 Ma) (Glodny et al., 2008; Melnick et al., 2009). Over geologic (millennial) timescales,  
 159 measured denudation rates in the region range between ~0.005 to ~0.6 mm yr<sup>-1</sup> (Schaller et al., 2018). To facilitate a comparison  
 160 between the study areas and focus on erosion variations from seasonal changes in precipitation and vegetation, we assume a  
 161 uniform rock uplift rate of 0.05 mm yr<sup>-1</sup> for this study. This rate is broadly consistent with the range of previously reported  
 162 values.

163 The climate gradient in the study areas ranges from an arid climate in Pan de Azúcar (north) with mean annual precipitation  
 164 (MAP) of ~11 mm yr<sup>-1</sup> to semi-arid in Santa Gracia (MAP: ~88 mm yr<sup>-1</sup>), a Mediterranean climate in La Campana (MAP:  
 165 ~350 mm yr<sup>-1</sup>), and a temperate-humid climate in Nahuelbuta (south) with a MAP of 1400 mm yr<sup>-1</sup> (Ziese et al., 2020). The  
 166 observed mean annual temperatures (MAT) also vary with latitude ranging from ~20°C in the north to ~5°C in the south  
 167 (Übernickel et al., 2020). The previous gradients in MAP and MAT and latitudinal variations in solar radiation result in a

Deleted: North

Deleted: South

Field Code Changed

Deleted: plate

Deleted: plate

Deleted: the

173 southward increase in vegetation density (Bernhard et al., 2018). The vegetation gradient is evident from mean MODIS  
174 Normalized Difference Vegetation Index (NDVI) values range from ~0.1 in Pan de Azúcar (north) to ~0.8 in Nahuelbuta  
175 (south) (Didan, Kamel, 2015). In this study, NDVI values are used as a proxy for vegetation cover density, similar to the  
176 approach of Schmid et al. (2018). However, one of the major limitations of using NDVI is that the values get saturated when  
177 the ground is covered by shrubs. This gradient in climate and vegetation cover from north to south in the Chilean Coastal  
178 Cordillera provides an opportunity to study the effects of seasonal variations in vegetation cover and precipitation on  
179 catchment-scale erosion rates in different environments.

180 **3 Methods**

181 This section comprises a description of model inputs (section 3.1), estimation of runoff rates (section 3.2), model setup (section  
182 3.3), and initial and boundary conditions (section 3.4). This is followed by an overview of simulations conducted (section 3.5),  
183 and a brief description of how detrending the model results was conducted to remove long-term transients (section 3.6).

184 **3.1 Data used for model inputs**

185 In contrast to previous modeling studies (Schmid et al., 2018; Sharma et al., 2021) in the same regions, we used present-day  
186 topography as the initial condition for simulations instead of a synthetic topography produced during a model spin-up phase  
187 in Landlab. This study focuses on predicting and comparing the average responses in catchment erosion that occur over  
188 seasonal timescales with variable precipitation and vegetation cover. However, erosion in arid and semi-arid regions can vary  
189 on sub-seasonal time scales due to high-intensity storms occurring over timescales of a couple of hours or days. Hence, the  
190 model does not capture the role of extreme precipitation events. The effect of vegetation on erosion during extreme events is  
191 the focus of ongoing work by the authors. Also, at seasonal time-steps, the relationship between vegetation cover and erosion  
192 rates may be affected by inherited simulated slope values from the previous season, which may lead to the blended signal in  
193 the output.

**Deleted:** LandLab.

194 Initial topography for the four selected catchments was obtained by cropping the SRTM digital elevation model (DEM) in  
195 rectangular shapes encapsulating the catchment of interest (Fig. 1). These catchments are the same as those investigated with  
196 previous soil, denudation, and geophysical studies within the EarthShape project (e.g., Bernhard et al., 2018; Oeser et al., 2018;  
197 Schaller et al., 2018; Dal Bo et al., 2019). The DEM has a spatial resolution of 90 m and is the same as the cell size used in  
198 the model (dx and dy) (SRTM data set of Earth Resources Observation And Science (EROS) Center, 2017). The present-day  
199 total relief in the catchments are ~1852 m in La Campana (~33 °S), followed by ~1063 m in Santa Gracia (~30 °S), ~809 m in  
200 Nahuelbuta (~38 °S) and ~623 m Pan de Azúcar (~26 °S). Investigated catchment sizes considered here vary between ~64 km<sup>2</sup>  
201 in Pan de Azúcar, ~142.5 km<sup>2</sup> in Santa Gracia, ~106.8 km<sup>2</sup> in La Campana, and ~68.7 km<sup>2</sup> in Nahuelbuta. We note that present-  
202 day topography as the initial condition in simulations can introduce an initial transience in erosion rates due to assumed model  
203 erosional parameters (e.g., erodibility, hillslope diffusivity) differing from actual parameters within the catchment. We address  
204 this issue through a detrending of model results described later (see Section 3.6). Also, topography and processes represented  
205 by LEMs have inherent timescales that they respond to base on the physical properties used and model forcings (e.g., rock  
206 uplift), which are unknown. Hence, it is unlikely that the SRTM DEM used for the initial condition, is in equilibrium. Given  
207 this, the detrending of our time series of results to remove long-term transience aids in identifying seasonal transients in  
208 precipitation and vegetation cover.

**Deleted:** /

**Deleted:** Maximum

**Deleted:** of

**Deleted:** is observed

**Deleted:** Catchment

**Deleted:** transient

**Deleted:** , we address this issue through a detrending of model results described later.

209 Precipitation data applied over each study area (Fig. 3b) was acquired from the Global Precipitation Climatology Centre  
210 (GPCC) for the period 01/03/2000 to 31/12/2019 (DD/MM/YEAR). The data has a spatial resolution of 1° and a 1-day temporal  
211 resolution and comprises daily land-surface precipitation from rain gauges built on Global Telecommunication System-based

222 and historic data (Ziese et al., 2020). The previous data was augmented with daily precipitation weather station data from  
223 01/02/2020 to 28/02/2020 obtained from Übernickel et al., (2020). We do this to include all the seasons between 2000 to 2019,  
224 i.e., from the austral autumn of 2000 to the austral summer of 2019. The periods (months of a year) of specific seasons in the  
225 Chilean Coastal Cordillera are given in Table 1. Seasonal precipitation rates were calculated by summing daily precipitation  
226 rates at three-month intervals. The seasonality and intensity of precipitation in the wet season (winter) increases from the arid  
227 (Pan de Azúcar) to humid temperate (Nahuelbuta) region.

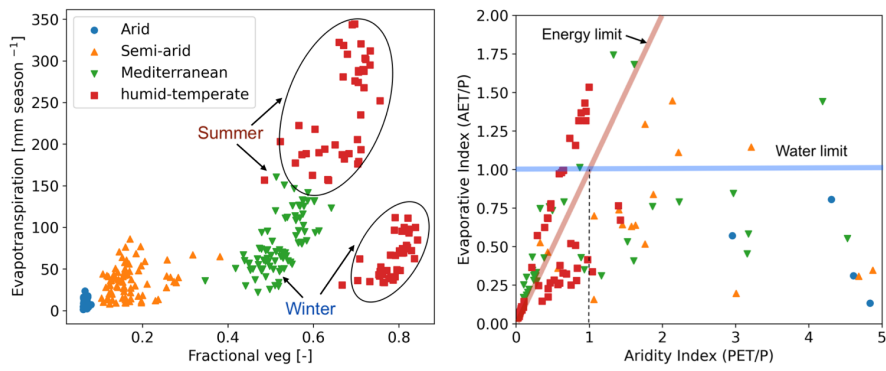
**Deleted:** Austral Autumn  
**Deleted:** Austral Summer  
**Deleted:** illustrated  
**Deleted:** up

228 **Table 1. Months of a year corresponding to specific seasons in the Chilean Coastal Cordillera**

Seasons	Months
Summer <sup>d*</sup>	December - February
Autumn <sup>w*</sup>	March - May
Winter <sup>w*</sup>	June - August
Spring <sup>d*</sup>	September - November

229 230 \*d: dry season, w: wet season

231 NDVI derived from remote sensing imagery has been proven as an effective tool to estimate seasonal changes in vegetation  
232 cover density (Garatuza-Payán et al., 2005). Normalized difference vegetation index (NDVI) values were obtained from  
233 MODIS (Didan, Kamel, 2015) satellite data and were used as a proxy for changes in vegetation cover in the catchments.  
234 However, the major limitation of the conversion of NDVI to vegetation cover includes a saturation problem in NDVI values  
235 that occurs in high biomass regions such as our humid-temperate setting (Huete et al., 2002). This saturation can occur if the  
236 ground is covered by shrubs, at which point the information on different plant communities for associated erosion-relevant  
237 properties is lost (e.g., rooting depth, etc.) The NDVI data were acquired for 20 years (01/03/2000 – 28/02/2020), with a  
238 spatial resolution of 250 m and temporal resolution of 16 days. For application within the model simulations, the vegetation  
239 cover dataset was resampled using the nearest neighbour method to match the spatial resolution (90 m) of SRTM DEM and  
240 temporal resolution of 3 months. To summarize, season variations in precipitation rate and vegetation cover were applied to  
241 the simulations between 01/03/2000 and 28/02/2020 and encompass a 20-year record of observation variations in these factors.  
242 Additional aspects of the catchment hydrologic cycle were determined using the following approaches for the same time period  
243 previously mentioned. First, evapotranspiration (ET) data was obtained from Global Land Data Assimilation System (GLDAS)  
244 Noah version 2.1, with a monthly temporal resolution and spatial resolution of 0.25° (~28 km) (Beaudoin et al., 2020; Rodell  
245 et al., 2004). The data was obtained from March-2000 to February-2020. Due to the coarse resolution of the dataset, ET is  
246 assumed to be uniform over the entire catchment area. No higher resolution datasets were available over the 20-year time-  
247 period of interest.  
248 Soil properties such as the grain size distribution (sand, silt, and clay fraction) and bulk density were adapted from Bernhard  
249 et al., (2018) to estimate soil water infiltration capacity in each study area. Based on these soil properties, the soils have been  
250 classified as a sandy loam (in Pan de Azúcar, Santa Gracia, and La Campana) and sandy clay loam (Nahuelbuta). Average  
251 bulk density values of 1300 kg m<sup>-3</sup>, 1500 kg m<sup>-3</sup>, 1300 kg m<sup>-3</sup>, and 800 kg m<sup>-3</sup> were used for Pan de Azúcar, Santa Gracia, La  
252 Campana, and Nahuelbuta, respectively (Bernhard et al., (2018).



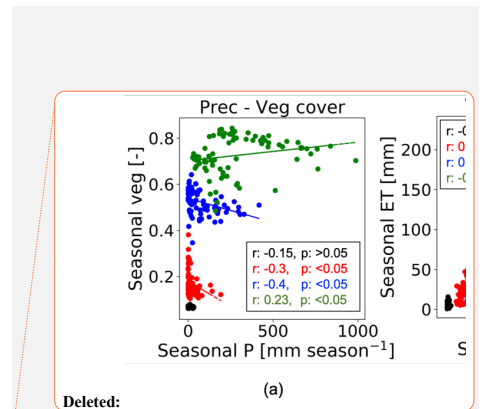
257  
258 **Figure 2.** Parameter correlation for observations used as model input data (i.e., seasonal precipitation, vegetation cover  
259 and evapotranspiration) including: (a) fractional vegetation cover (derived from NDVI) and evapotranspiration  
260 (derived from GLDAS NOAH), (b) Budyko curve representing the relationship between precipitation (P), potential  
261 evapotranspiration (PET) and actual transpiration (AET). The points above the water limit (blue line) indicate the  
262 contribution of soil moisture to ET. The points above the energy limit (red line) indicate the precipitation loss  
263 by infiltration. The plots represent observations corresponding to Autumn of 2000 to Summer of 2019. Each data point  
264 represents one season and are color coded by climate of the study areas. See section 3.1 for a description of the data  
265 sets used.

266 Figure 2 shows correlations between the model input data, such as variable climatic or hydrologic cycle metrics (i.e.,  
267 precipitation and evapotranspiration) and vegetation cover for the climate of each study area investigated. The relationships  
268 shown for each area in different climate-ecological zones are based on the 20 years of data used (i.e., Autumn of 2000 –  
269 Summer of 2019). The relationship between fractional vegetation cover (V) and evapotranspiration (ET) indicates a slightly  
270 positive trend in the semi-arid setting (Fig. 2a). Whereas, the relationship in the Mediterranean setting is a steep positive  
271 gradient, with low vegetation cover (0.4–0.55) and evapotranspiration (i.e., 50–100 mm season<sup>-1</sup>) in the winter, which  
272 increases in summer (90–160 mm season<sup>-1</sup>) in response to vegetation growth (i.e., V = 0.55–0.65). Similar trends in V and  
273 ET is indicated in the humid temperate setting during the summer with V in the range of 0.55–0.75 and ET ranging between  
274 150–350 mm season<sup>-1</sup>. However, during winters, even after high V in humid setting, lower values in ET are reported, with a  
275 positive trend. To help understand the datasets of precipitation (P) with ET, a Budyko curve is presented in figure 2b, where  
276 the actual ET (AET) and potential ET (PET) are normalized by P. In figure 2b most the data points from the humid temperate  
277 setting are above the energy limit and indicate high soil water infiltration during summer seasons. Also, data points above the  
278 water limit (blue line in Fig. 2b) indicate a carry-over in soil moisture from a wet season to few dry seasons in the humid,  
279 Mediterranean and semi-arid settings.

### 280 3.2 Estimation of runoff rates

281 The precipitation rates [m season<sup>-1</sup>] are subjected to soil-water infiltration [m season<sup>-1</sup>] and evapotranspiration [m season<sup>-1</sup>] to  
282 estimate the seasonal runoff rates [mm season<sup>-1</sup>]. The runoff rates (R) at every time step (t) are calculated using the actual soil-  
283 water infiltration ( $I_a$ ) and the actual evapotranspiration (ET) as follows,

$$284 R(t) = P(t) - I_a(t) - ET(t) \quad (1)$$



Deleted: seasonal precipitation [mm season<sup>-1</sup>] and fraction of vegetation cover [-]. (b) fractional seasonal vegetation cover [-] and evapotranspiration [mm], and (c) seasonal precipitation [mm season<sup>-1</sup>] and evapotranspiration [mm].

Deleted: study area (AZ: Pan de Azúcar, SG: Santa Gracia, LC: La Campana, and NA: Nahuelbuta).

Deleted: Figure 2 shows correlations between the model input data, such as variable climatic or hydrologic cycle metrics (i.e., precipitation and evapotranspiration) and vegetation cover for each study area investigated. The relationships, and regression lines, shown for each area in different climate-ecological zones the general seasonal relationships over the 20 years (i.e., Autumn of 2000 – Summer of 2019) of data. For example, the correlation between seasonal precipitation and vegetation cover (Fig. 2a) illustrates a moderate negative correlation ( $r > -0.4$ ) in the semi-arid (SG) and Mediterranean (LC) regions. In contrast, vegetation in the humid temperate region (NA) is positively correlated ( $r: 0.23$ ). ET and vegetation cover are positively correlated (Fig. 2b) in the semi-arid (SG) and Mediterranean regions (LC). However, the correlations are negative in the humid-temperate region (NA). The correlation between seasonal precipitation and ET (Fig. 2c) is slightly positive ( $r: -0.2$ ) in the semi-arid region (SG) and moderately negative ( $r: -0.4$ ) in the Mediterranean (LC) study area. However, we observe a strong negative correlation ( $r: -0.8$ ) between precipitation and ET in humid-temperate and Mediterranean regions (LC and NA, Fig. 2c). This negative correlation is owed to the steep negative gradient in temperature (e.g., ~2.5 °C in NA) and solar radiation (Übernickel et al., 2020) during winters (wet season) in southern latitudes (LC and NA).<sup>¶</sup>

317 where,  $P$  is the precipitation amount in a season. This relationship was applied in the model grid cells with non-zero sediment  
318 thickness. As ET is the input parameter, there may be instances of higher ET than P in the summer seasons in the humid,  
319 Mediterranean and semi-arid settings. This is evident in figure 2b where the minimum of both values is used as ET in the given  
320 time-step.

321 The soil-water infiltration rate was estimated by applying the Green-Ampt equation (Green and Ampt, 1911; Julien et al.,  
322 1995):

$$f(t) = K_e \left( 1 + \frac{\Psi \Delta \theta}{F} \right)^{-1} \quad (2)$$

324 where  $f(t)$  is the infiltration rate [ $\text{m s}^{-1}$ ] at time  $t$ ,  $K_e$  is the effective hydraulic conductivity [ $\text{m s}^{-1}$ ],  $F$  is the cumulative infiltration  
325 [m],  $\Psi$  is the suction at the wetting front [m], and  $\Delta \theta$  is the difference between saturated and initial volumetric moisture content  
326 [ $\text{m}^3 \text{ m}^{-3}$ ]. Effective hydraulic conductivity is highly variable and anisotropic; hence, it was considered to be uniform with a  
327 value of  $1 \times 10^{-6} \text{ m s}^{-1}$  for each catchment.

328 Following the approach of Istanbulluoglu and Bras, (2006) for loamy soils, the soil-water infiltration was modified to account  
329 for variable vegetation cover in each grid cell, as follows:

$$I_c(t) = f(t)(1 - V(t)) + 4f(t)(V(t)), \quad (3)$$

$$I_a(t) = \min[P(t), I_c(t)], \quad (4)$$

332 where  $I_c$  is the infiltration capacity and  $V$  is the vegetation cover (between 0 and 1) in a model grid cell at time-step  $t$ . Values  
333 used in the simulations for the parameters in equations 2-4 are provided in appendix Table A1.

### 334 3.3 Model setup

335 We applied the Landlab landscape evolution model, a python-based modeling toolkit (Hobley et al., 2017), combined with the  
336 SPACE 1.0 model (Shobe et al., 2017). The SPACE model allows coupled detachment-transport limited fluvial processes with  
337 simultaneous bedrock erosion and sediment entrainment/deposition. The Landlab-SPACE programs were applied using a set  
338 of runtime scripts and input files (Sharma and Ehlers, 2023) to account for vegetation and climate change effects on catchment  
339 erosion (i.e., fluvial erosion and hillslope diffusion), using the approach described in Schmid et al. (2018) and Sharma et al.  
340 (2021). In addition, the geomorphic processes considered involve weathering and regolith production (Barnhart et al., 2019)  
341 and infiltration of surface water into soil (Rengers et al., 2016) based on the Green-Ampt method (Green and Ampt, 1911),  
342 and runoff modeling.

343 The model parameters (Table. A1) are selected for the distinct climate and ecological settings in the Chilean Coastal Cordillera  
344 based on the observations presented in Schaller et al., (2018). The model state parameters (i.e., erodibility, diffusivity, rock  
345 uplift rate, etc.) in the simulations are adapted from Sharma et al., (2021). The model was simulated at a seasonal scale (time  
346 step of three months) from the autumn of 2000 (01/03/2000) to the summer of 2019 (28/02/2020). Simulations were conducted  
347 for a total time of 1000 years with a time-step of 1 season (3 months) with 20 years (2000 – 2019) of observations in vegetation  
348 and precipitation. These 20-years of observations were repeated (looped) 50 times, to identify, and detrend, long-term transient  
349 trends in catchment erosion rates due to potential differences in actual and assumed erosional parameters such as the hillslope  
350 diffusivity or fluvial erodibility. The combined effects of temporally variable (at seasonal scale) precipitation and vegetation  
351 cover (also spatially variable) on catchment-scale erosion rates are therefore the primary factors influencing predicted erosion  
352 rates.

**Deleted:** module of Shobe et al. (2017). The SPACE module  
**Deleted:** modified for vegetation-dependent hillslope processes (Johnstone and Hilly, 2014) and vegetation-dependent overland flow and fluvial erosion using the approach described in Schmid et al.

**Deleted:** calibrated to

**Deleted:** of

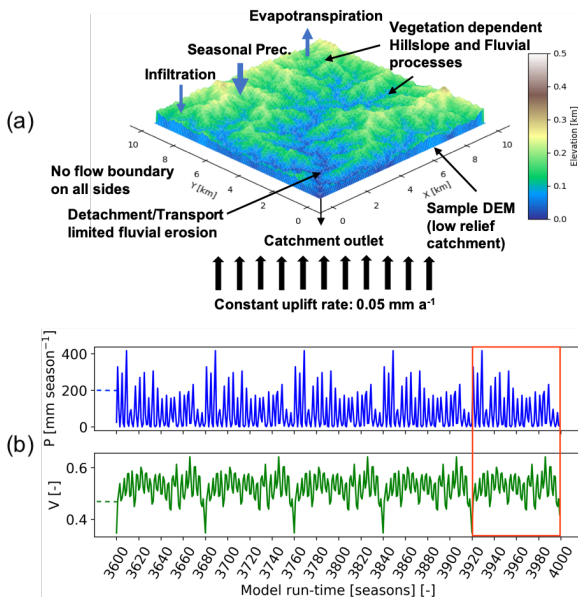
**Deleted:** erosion, diffusion, lithology, tectonic

**Deleted:** Autumn

**Deleted:** Summer

**Deleted:** effect

**Deleted:** was



365  
366 **Figure 3. Schematic of the model geometry and seasonal precipitation and vegetation forcings used in this study.** (a)  
367 Model setup representing sample DEM (low relief catchment) with no flow boundaries on all sides and a single  
368 catchment outlet. The model involves vegetation-dependent seasonal hillslope and fluvial processes and rainfall-  
369 infiltration-runoff modeling. (b) Seasonal precipitation and vegetation cover dataset (Mediterranean, La Campana,  
370 setting) for the last five iterations of model simulations. The results of highlighted iterations (after detrending for long-  
371 term transients) are analyzed in consecutive sections.

372 **3.4 Boundary and initial conditions**

373 The boundaries are closed (no flow) on all sides, with a single stream outlet at the point of minimum elevation at boundary  
374 nodes (Fig. 3). Initial sediment cover thickness is considered uniform across the model domain, and was approximated based  
375 on observations by Schaller et al., (2018) and Dal Bo et al., (2019). The sediment thickness used are 0.2 m in the arid (AZ),  
376 0.45 m in semi-arid (SG), 0.6 m in the Mediterranean (LC), and 0.7 m in humid temperate (NA) catchments. The rock uplift  
377 rate is kept constant throughout the entire model run as 0.05 mm yr<sup>-1</sup>, adapted from a similar study (Sharma et al., 2021).

**Deleted:** initial

378 **3.5 Overview of simulations conducted**

379 The simulations were designed to identify the sensitivity of erosion rates to seasonal variations in either precipitation rates or  
380 vegetation cover, as well as the more realistic scenario of coupled seasonal variations in both vegetation cover and  
381 precipitation. We evaluated this sensitivity with a step-wise increase in model complexity. Three sets of simulations were  
382 designed for the four selected study areas, which are as follows,

- 383 1. Scenario 1: Influence of constant (mean seasonal) precipitation with seasonal variations in vegetation cover  
384 catchment-scale erosion rates.

386        2. Scenario 2: Influence of seasonal variation in precipitation and constant (mean seasonal) vegetation cover on  
 387              catchment-scale erosion rates.  
 388        3. Scenario 3: Influence of coupled seasonal variations in both precipitation and vegetation cover on catchment-scale  
 389              erosion rates.  
 390        The results for scenarios 1 – 3 are illustrated in sections 4.1, 4.2, and 4.3, respectively.

### 3.6 Detrending of results for long term transients

### 3.6 Detrending of results for long term transients

Model simulations were conducted for 1,000 years using 20 years [March-2000 – Feb-2020] of observations in vegetation cover, and precipitation and were repeated 50 times for a total simulation duration of 1000 years. Simulations presented here were conducted on the present-day topography to allow for the application of observed time series of precipitation and vegetation change in different ecosystems and study areas. This choice of setting comes with the compromise that the erosional parameters (e.g., diffusivity, erodibility, etc.) used in the model are likely not the same as those that led to the present-day catchment topography. As a result, a long-term transient in erosion rates is expected as the model tries to reach an equilibrium with assumed erosional parameters. To correct for any long-term transients in erosion influencing our interpretations, we conducted a linear detrending of the results to remove any long-term variations. The detrending was conducted through a linear regression over entire time series of 1000 years and the values were corrected using the slope of the regression line. Hence, the detrended model results for the last 20 years were analyzed and discussed in sections 4 and 5. In practice, the detrending of time series did not impart a significant change to the results presented.

403 **4 Results**

404 In the following sections, we focus our analysis on the mean catchment erosion rates over seasonal (3 months) time scales (see  
 405 Table 1). In all scenarios, the rock uplift rate was kept constant at  $0.05 \text{ mm yr}^{-1}$  following the approach of Sharma et al. (2021).  
 406 For simple representation, the results of the last five years of the last cycle of transient simulations starting from Autumn-2015  
 407 to Summer-2019 are displayed in Fig. 4, 6, and 8 (after detrending, see section 3.6). The results for the entire time series  
 408 (Autumn-2000 – Summer-2019) are available in the supplement (Fig. 1 – 3). The precipitation and erosion rates are shown  
 409 with the units [ $\text{mm season}^{-1}$ ].

#### 4.1 Scenario 1: Influence of constant precipitation and seasonal variations in vegetation cover on erosion rates

In scenario 1, vegetation cover (MODIS NDVI from March 2000 to February 2020) fluctuates seasonally (Fig. 4b), and precipitation rates are kept constant at the seasonal mean (i.e., MAP divided by the number of seasons in a year) during the entire time-series (Fig. 4a) (Ziese et al., 2020). The range of seasonal vegetation cover variations (and mean seasonal precipitation rates) are observed as  $0.06 - 0.08$  ( $3.92 \text{ mm season}^{-1}$ ),  $0.1 - 0.4$  ( $20.16 \text{ mm season}^{-1}$ ),  $0.35 - 0.65$  ( $79 \text{ mm season}^{-1}$ ), and  $0.5 - 0.85$  ( $292 \text{ mm season}^{-1}$ ) for the arid, semi-arid, Mediterranean and, humid temperate settings, respectively (Figs. 4a-b). The predicted mean catchment seasonal erosion rates range between  $0 - 6 \times 10^{-4} \text{ mm season}^{-1}$ ,  $0 - 9.4 \times 10^{-4} \text{ mm season}^{-1}$ ,  $0 - 2.3 \times 10^{-3} \text{ mm season}^{-1}$ , and  $1.2 \times 10^{-3} - 4 \times 10^{-3} \text{ mm season}^{-1}$  for the arid, semi-arid, Mediterranean and humid temperate settings, respectively (Fig. 4c).

To analyze the relationships between the relative changes in forcings and responses, seasonal changes in vegetation cover and erosion rates were normalized between 0 and 1 and plotted in Figs. 5a-d. An inverse relationship and negative correlation (Kendall-tau correlation coefficient: 0.4–0.5) is visible between the normalized catchment erosion rates and vegetation cover for the dry season and wet season separately in the humid temperate (Fig. 5d) and Mediterranean settings (Fig. 5c). The linear relationship in vegetation and erosion change in the Mediterranean and humid-temperate settings indicates that these

## Moved (insertion) [1]

**Deleted:** 4a) (Ziese et al., 2020). The range of seasonal vegetation cover variations (and mean seasonal precipitation rates) are observed as 0.06 – 0.08 [-] (3.92 mm season<sup>-1</sup>), 0.1 – 0.4 [-] (20.16 mm season<sup>-1</sup>), 0.35 – 0.65 [-] (79 mm season<sup>-1</sup>), and 0.5 – 0.85 [-] (292 mm season<sup>-1</sup>) for the Pan de Azúcar, Santa Gracia, La Campana and Nahuelbuta study areas (Fig. 1), respectively.

**Deleted:** The predicted mean catchment

**Deleted:** range between  $0 - 6 \times 10^{-4}$  mm season $^{-1}$ ,  $0 - 9.4 \times 10^{-4}$  mm season $^{-1}$ ,  $0 - 2.3 \times 10^{-3}$  mm season $^{-1}$ , and  $1.2 \times 10^{-3} - 4 \times 10^{-3}$  mm season $^{-1}$  in Pan de Azúcar, Santa Gracia, La Campana, and Nahuelbuta, respectively (Fig.

**Moved up [1]: 4c).**

**Deleted:** The mean catchment seasonal

**Deleted:** have an inverse linear relationship with seasonal

**Deleted:** arid, semi-arid,

**Deleted:** 5) However, this relationship is positive in the humid-temperate setting, i.e., erosion increases with an increase in vegetation cover with a relatively lower gradient ( $3 \times 10^{-3}$ ).  
This is in contrast to the

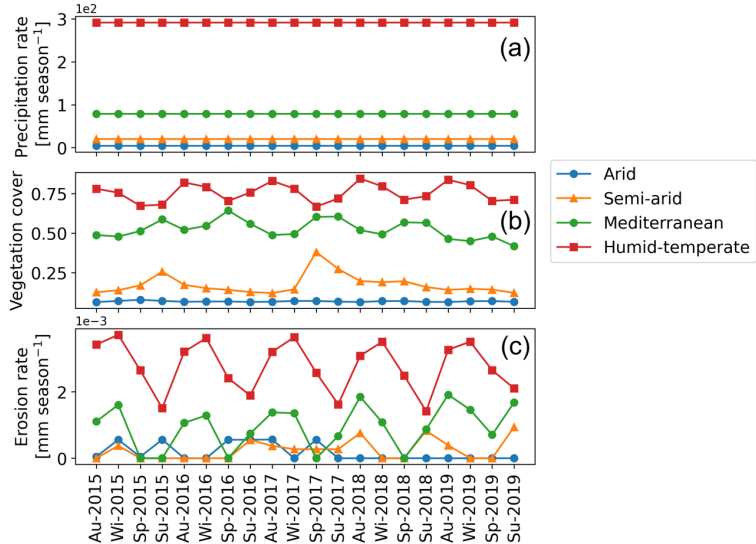
**Deleted cases**

### **Deleted: cover**

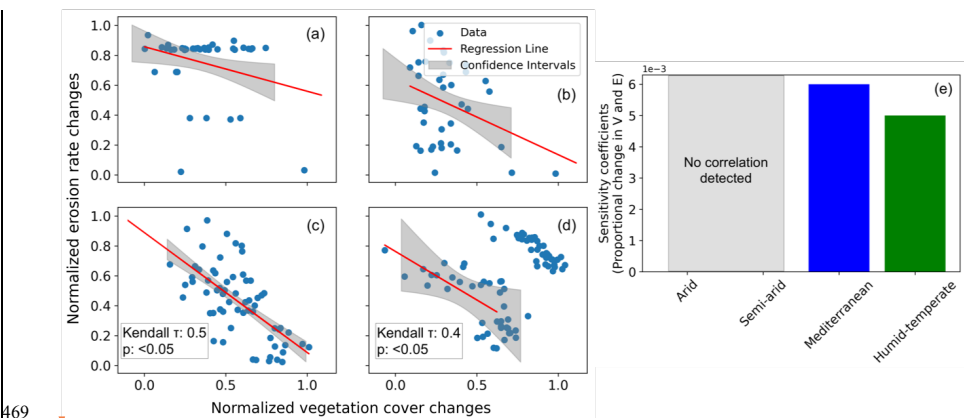
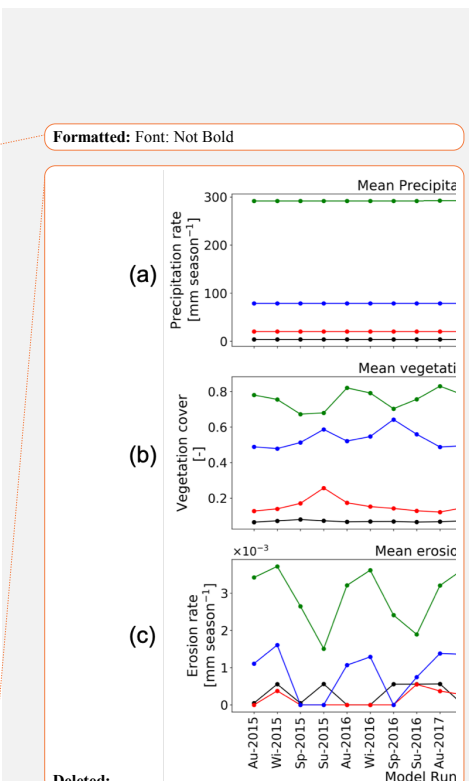
**Deleted:** rates is observed

**Deleted:** The Mediterranean region (La Campana) is ~4.5 times more sensitive than the semi-arid region (Santa Gracia). Due to very low precipitation in the arid region (Pan de Azúcar), no significant range in erosion rates is observed (e.g., Pearson  $r$ : 0.17;  $p$ : >0.05). The results (Fig. 4 and 5) suggest a high sensitivity in erosion in the Mediterranean setting to changes in seasonal vegetation cover (i.e., erosion rates decrease with an increase in vegetation cover). The erosion rates are low (e.g., <0.005 mm season $^{-1}$ ) due to low mean precipitation rates subjected to infiltration and evapotranspiration.

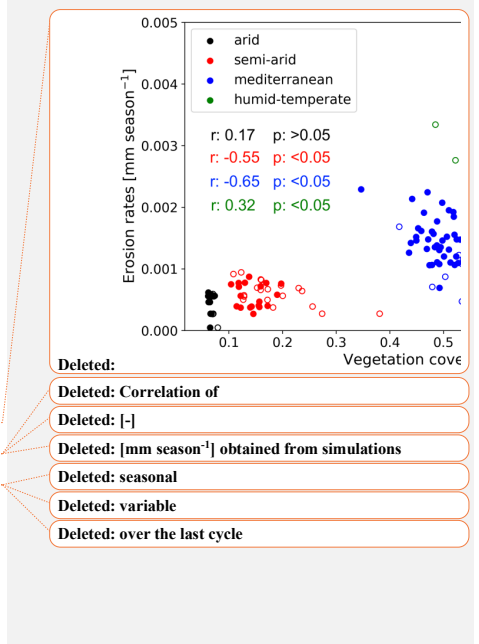
462 catchments are dominated by fluvial (water driven) and overland flow processes, and the role of hillslope diffusion is minimal.  
 463 In contrast, no correlation was found for the arid and semi-arid settings.



464  
 465 **Figure 4.** Results of simulations with constant seasonal precipitation and variable vegetation over last 5 years (Autumn-  
 466 2015 – Summer-2019) of last cycle of transient-state model run representing: (a) mean catchment seasonal precipitation  
 467 rates [mm season<sup>-1</sup>], (b) mean catchment seasonal vegetation cover [-], and (c) mean catchment seasonal erosion rates  
 468 [mm season<sup>-1</sup>].



469  
 470 **Figure 5.** Seasonal changes (normalized) in vegetation cover and erosion rates for the scenario with constant  
 471 precipitation and seasonal changes in vegetation cover in (a) arid, (b) semi-arid, (c) Mediterranean, and (d) humid-  
 472 temperate settings, with the information on confidence interval (grey shading) and Kendall-tau correlation coefficients.



481 (e) Sensitivity coefficients for proportional changes in vegetation cover and erosion rates based on the slope and  
 482 intercept of the regression lines for the above environmental settings. The sensitivity coefficient is defined as the slope  
 483 of the regression line presented in sub-sections a-d.

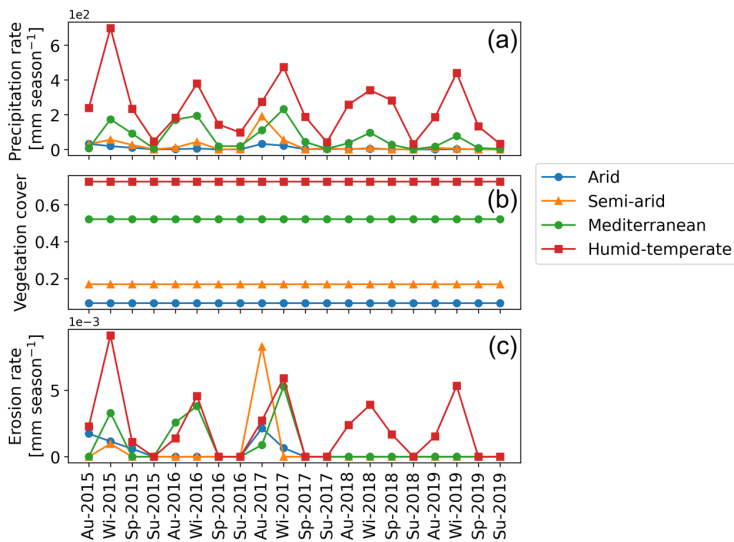
484 The sensitivity coefficients based on slope and intercept of the regression lines (Figs. 5a-d) are plotted in Fig. 5e. The results  
 485 indicate a higher sensitivity of erosion rates to seasonal vegetation changes in the Mediterranean setting relative to humid-  
 486 temperate setting. However, in the arid and semi-arid settings, the lack of a significant correlation in the change in vegetation  
 487 cover and erosion rates leads to a low sensitivity. This is owed to very low mean precipitation rates ( $<20 \text{ mm season}^{-1}$ ) in the  
 488 arid and semi-arid settings. The predicted erosion rates are relatively low (e.g.,  $<0.004 \text{ mm season}^{-1}$ ) in this scenario, due to  
 489 low mean precipitation rates, which are primarily subjected to infiltration and evapotranspiration in these drier settings.

Deleted: transient state model run (Autumn-2000 – Summer-2019). Hollow circles: dry season; filled circles: wet season. Each individual circle represents one  
 Formatted: Space After: 0 pt

#### 490 4.2 Scenario 2: Influence of seasonal variations in precipitation and constant vegetation cover on erosion rates

491 In scenario 2, vegetation cover (MODIS NDVI from Mar-2000 – Feb-2020) is kept constant at the mean seasonal vegetation  
 492 cover (Fig. 6b) and precipitation rates vary seasonally (Mar-2000 – Feb-2020) (Fig. 6a). The range of seasonal precipitation  
 493 rate variations are observed in the range of  $0 – 32.42 \text{ mm season}^{-1}$ ,  $0 – 191.66 \text{ mm season}^{-1}$ ,  $0.03 – 417 \text{ mm season}^{-1}$ , and  $26 – 987 \text{ mm season}^{-1}$   
 494 in the arid, semi-arid, Mediterranean and, humid temperate settings, respectively.

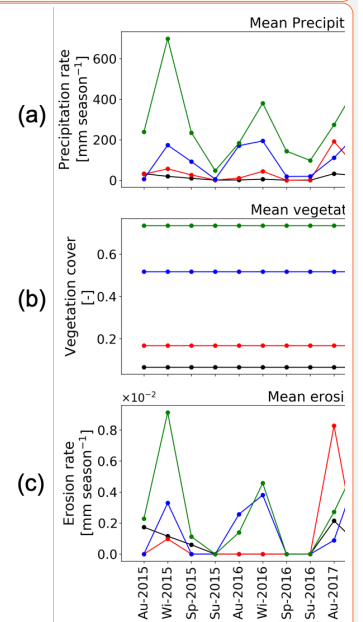
495 The simulated mean catchment seasonal erosion rates are observed in the range of  $0 – 2 \times 10^{-3} \text{ mm season}^{-1}$ ,  $0 – 8.3 \times 10^{-3} \text{ mm season}^{-1}$ ,  
 496  $0 – 1.37 \times 10^{-2} \text{ mm season}^{-1}$ , and  $0 – 1.3 \times 10^{-2} \text{ mm season}^{-1}$  in the arid, semi-arid, Mediterranean and, humid  
 497 temperate settings, respectively (Fig. 6c).



498  
 499 Figure 6. Results of simulations with variable seasonal precipitation and constant vegetation over last 5 years (Autumn-  
 500 2015 – Summer-2019) of last cycle of transient-state model run representing: (a) mean catchment seasonal precipitation  
 501 rates [ $\text{mm season}^{-1}$ ], (b) mean catchment seasonal vegetation cover [-], and (c) mean catchment seasonal erosion rates  
 502 [ $\text{mm season}^{-1}$ ].

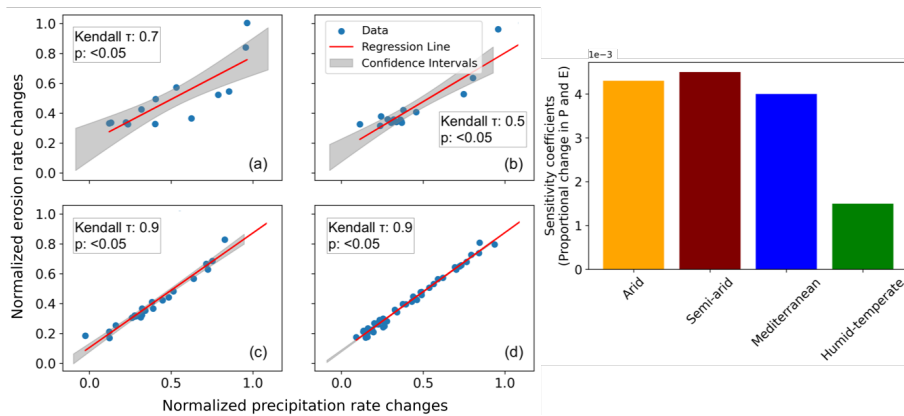
Deleted: season within the timeseries  
 Formatted: Font: Not Bold  
 Formatted: Font: Not Bold, Not Italic  
 Formatted: Font: Not Bold

Deleted: for Pan de Azúcar, Santa Gracia, La Campana and Nahuelbuta



Deleted:  
 Moved (insertion) [2]  
 Moved (insertion) [3]

510 Similar to scenario 1, the changes in seasonal precipitation and erosion rates were normalized between 0 and 1 and plotted in  
 511 Figs. 7a-d. A strong positive correlation (Kendall-tau correlation coefficient ranging from 0.5 in semi-arid to 0.9 in  
 512 Mediterranean and humid-temperate settings) in the normalized precipitation and erosion rates changes is predicted with the  
 513 majority of the data points within the 95% confidence interval in all the settings. The sensitivity coefficients based on the  
 514 proportional changes in precipitation and erosion rates, indicate the highest sensitivity in semi-arid settings with ~5%, ~11%  
 515 and ~67% lower sensitivities in the arid, Mediterranean, and humid-temperate settings, respectively (Fig. 7e). This may be  
 516 owed to the occasional El Niño events with extremely high precipitation occurring in the arid and semi-arid settings (with  
 517 sparse vegetation cover).



518  
 519 **Figure 7.** Seasonal changes (normalized) in precipitation and erosion rates for the scenario with seasonal changes in  
 520 precipitation rates and constant vegetation cover in (a) arid, (b) semi-arid, (c) Mediterranean, and (d) humid-temperate  
 521 settings, with the information on confidence interval (grey shading) and Kendall-tau correlation coefficients.  
 522 (e) Sensitivity coefficients for proportional changes in precipitation and erosion rates based on the slope and intercept of  
 523 the regression lines for the above environmental settings. The sensitivity coefficient is defined as the slope of the  
 524 regression line presented in sub-sections a-d.

525 **4.3 Scenario 3: Influence of coupled seasonal variations in both precipitation and vegetation cover on erosion rates**  
 526 In this scenario, coupled variations in seasonal vegetation cover (MODIS NDVI from Mar-2000 – Feb-2020) (Fig. 8b) and  
 527 precipitation rates are presented for the years 2000 - 2019 (Fig. 8a). The range of seasonal precipitation rates (and seasonal  
 528 vegetation cover, V) variations are 0 – 32.42 mm season<sup>-1</sup> (V= 0.06 – 0.08), 0 – 191.66 mm season<sup>-1</sup> (0.1 – 0.38), 0.03 – 417  
 529 mm season<sup>-1</sup> (0.35 – 0.65), and 26 – 987 mm season<sup>-1</sup> (0.5 – 0.85) in the arid, semi-arid, Mediterranean and humid temperate  
 530 settings, respectively (Figs. 8a-b). The mean catchment seasonal erosion rates range between 0 – 2 × 10<sup>-3</sup> mm season<sup>-1</sup>, 0 –  
 531 1 × 10<sup>-2</sup> mm season<sup>-1</sup>, 0 – 1.4 × 10<sup>-2</sup> mm season<sup>-1</sup>, and 0 – 1.4 × 10<sup>-2</sup> mm season<sup>-1</sup> in the arid, semi-arid, Mediterranean  
 532 and humid temperate settings, respectively (Fig. 8c).  
 533 Changes in precipitation on erosion rates were normalized between 0 and 1 and plotted in figures 9a-d. Similar to the results  
 534 from scenario 2, a strong positive correlation was predicted in all the environmental settings. The sensitivity coefficients based  
 535 on the proportional changes in precipitation and erosion rates, indicate the highest sensitivity in the semi-arid settings with  
 536 ~25% and ~71% lower sensitivities in arid and Mediterranean and humid-temperate settings, respectively (Fig. 9e). Similarly,  
 537 the isolated effect of changes in the vegetation cover on erosion rates (Fig. 10) does not yield a significant correlation in

**Moved up [2]:** The simulated mean catchment seasonal erosion rates are observed in the range of 0 – 2 × 10<sup>-3</sup> mm season<sup>-1</sup>, 0 – 8.3 × 10<sup>-3</sup> mm season<sup>-1</sup>, 0 – 1.37 × 10<sup>-2</sup> mm season<sup>-1</sup>, and 0 – 1.3 × 10<sup>-2</sup> mm season<sup>-1</sup> in

**Moved up [3]:** 6c).

**Deleted:** Pan de Azúcar, Santa Gracia, La Campana, and Nahuelbuta, respectively (Fig.

**Deleted:** The mean catchment seasonal erosion rates are positively correlated with seasonal precipitation rates (Fig. 7), with a maximum gradient in the arid region (AZ, gradient: ~1.3 × 10<sup>-4</sup>). The gradients in the precipitation – erosion rate relationship (Fig. 7) indicate the sensitivity of each catchment

**Deleted:** rates, such that that the arid region (AZ) is ~2.7, ~3.2,

**Deleted:** ~8 times more sensitive than

**Deleted:** (SG),

**Deleted:** (LC)

**Deleted:** region (NA), respectively. The results (Fig. 6

**Deleted:** 7) suggest a high sensitivity of erosion

**Moved (insertion) [4]**

**Deleted:** to changes in seasonal precipitation rates (i.e., erosion increases at relatively higher rates with an increase

**Formatted:** Font: Bold

**Deleted:** ). The erosion rates are higher than in scenario 1 (e.g., 0 – 0.014 mm season<sup>-1</sup>) due to higher precipitation rates

**Deleted:** 2.¶ ... [2]

**Formatted:** Font: Bold

**Moved up [4]:** Figure 7.

**Formatted**

**Deleted:** Correlation of precipitation rates [mm season<sup>-1</sup>]

**Deleted:** [-],

**Deleted:** [-],

**Deleted:** [-],

**Deleted:** [-] for Pan de Azúcar, Santa Gracia, La Campana

**Deleted:** Nahuelbuta

**Moved (insertion) [5]**

**Deleted:** .

**Deleted:** The mean catchment seasonal erosion rates are ...

**Deleted:** the range of 0 – 2 × 10<sup>-3</sup> mm season<sup>-1</sup>, 0 – ...

**Moved up [5]:** 8c).

**Deleted:** Similar to scenario 2, mean catchment seasonal ...

**Deleted:** rates (Fig. 9), with a maximum gradient in an arid ...

**Deleted:** – erosion rate relationship (Fig. 9) represent the ...

**Deleted:** vegetation cover. The results (Fig. 8 and 9)

**Deleted:** that

**Deleted:** arid region (AZ) is ~2.3, ~3, and ~8 times more

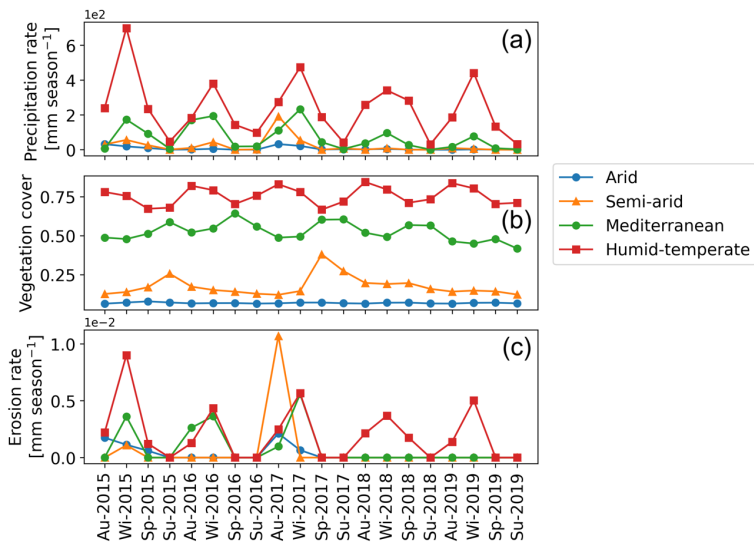
**Deleted:** (SG),

**Deleted:** (LC),

**Deleted:** region (NA), respectively.

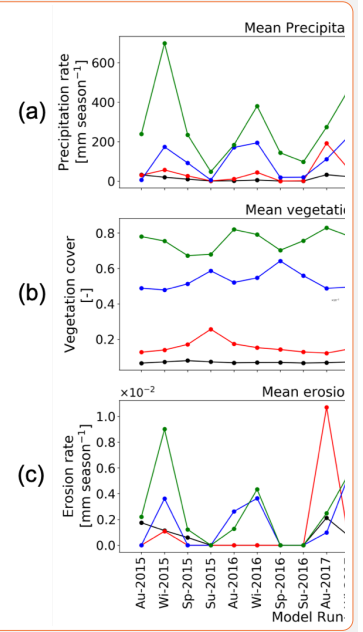
612 arid, semi-arid and Mediterranean settings. However, we observe a strong negative correlation in the humid-temperate setting  
 613 (Fig. 10d) during the wet season (Kendall tau correlation coefficient: -0.6, with >95% significance level). Hence, the sensitivity  
 614 coefficients in this case are not plotted.

615 The similarity in results obtained from scenarios 2 and 3 suggest a first-order control of seasonal precipitation changes on  
 616 erosion rates (~70% higher sensitivity to changes in precipitation), with less significance to vegetation cover changes. For  
 617 example, the sensitivity of erosion to precipitation rate changes in semi-arid setting is predicted as ~70% higher to that of  
 618 humid-temperate setting in both the scenarios.

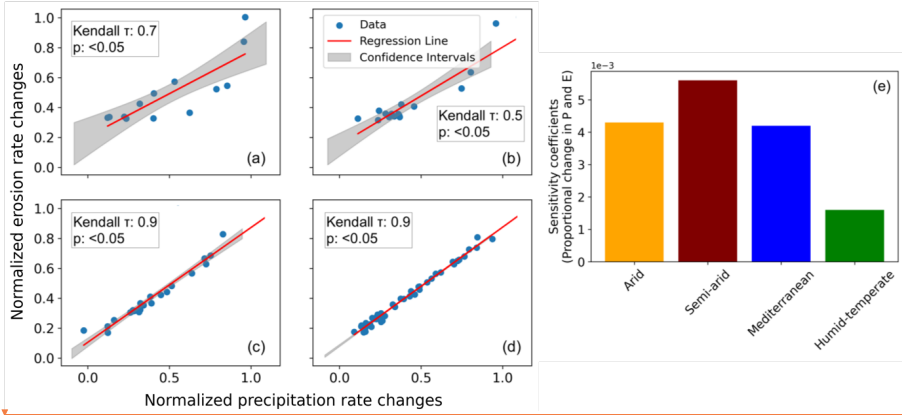


620  
 621 **Figure 8.** Results of simulations with coupled variations in seasonal precipitation and vegetation over the last five years  
 622 (Autumn-2015 – Summer-2019) of the last cycle of transient-state model run representing: (a) mean catchment seasonal  
 623 precipitation rates [ $\text{mm season}^{-1}$ ], (b) mean catchment seasonal vegetation cover [-], and (c) mean catchment seasonal  
 624 erosion rates [ $\text{mm season}^{-1}$ ].

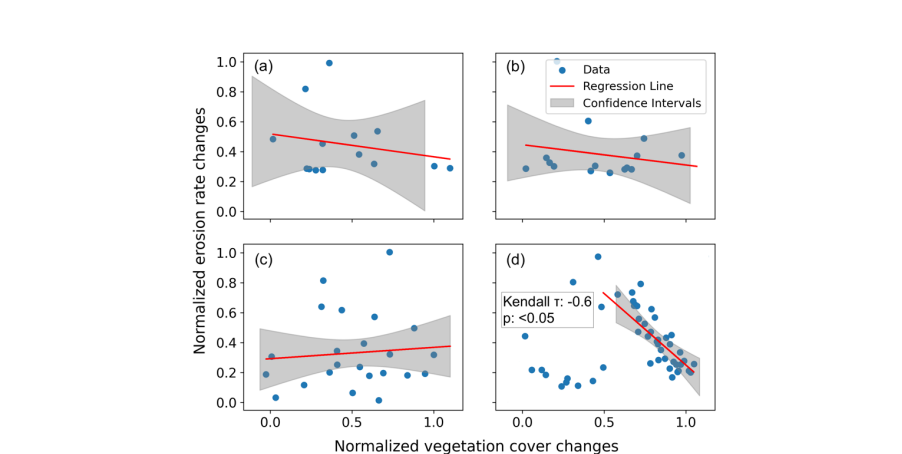
**Deleted:** the  
**Deleted:** (e.g., Pearson  $r > 0.6$  for arid setting, Fig. 9a  
**Deleted:** changing  
**Deleted:** (Pearson  $r < -0.19$  for  
**Deleted:** , Fig. 9b).



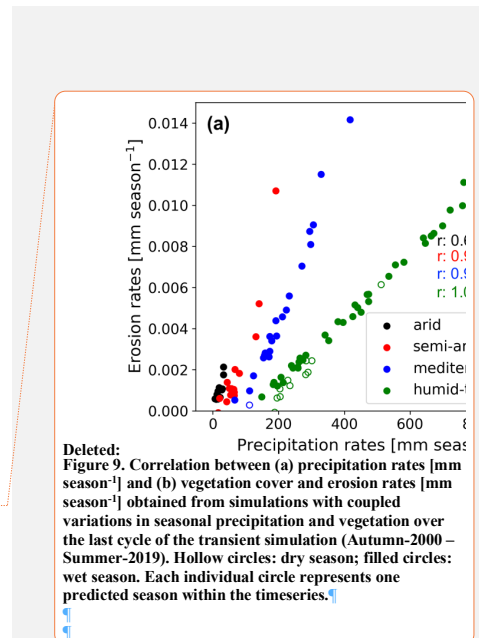
Deleted:



631  
632 [Figure 9. Seasonal changes \(normalized\) in precipitation and erosion rates for the scenario with coupled seasonal](#)  
633 [changes in both precipitation rates and vegetation cover in \(a\) arid, \(b\) semi-arid, \(c\) Mediterranean, and \(d\) humid-](#)  
634 [temperate settings, with the information on confidence interval \(grey shading\) and Kendall-tau correlation coefficients.](#)  
635 [\(e\) Sensitivity coefficients for proportional changes in precipitation and erosion rates based on the slope and intercept](#)  
636 [of the regression lines for the above environmental settings. The sensitivity coefficient is defined as the slope of the](#)  
637 [regression line presented in sub-sections a-d.](#)



639  
640 [Figure 10. Seasonal changes \(normalized\) in vegetation cover and erosion rates for the scenario with coupled seasonal](#)  
641 [changes in both precipitation rates and vegetation cover in \(a\) arid, \(b\) semi-arid, \(c\) Mediterranean, and \(d\) humid-](#)  
642 [temperate settings, with the information on confidence interval \(grey shading\) and Kendall-tau correlation coefficients.](#)



655 

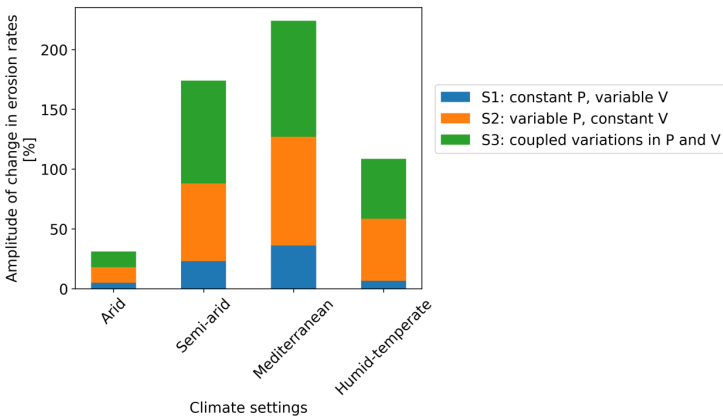
## 5 Discussion

656 This section discusses the relationship between variations in seasonal precipitation and vegetation cover with erosion rates in  
 657 the form of the amplitude of change for each model scenario (section 5.1). This is followed by the synthesis of catchment scale  
 658 erosion rates variability over wet and dry seasons (section 5.2). In section 5.3, we discuss the impact transient dynamics of  
 659 sediment transport in our modelling approach. Finally, we compare our results with previously published studies (section 5.4)  
 660 and discuss model limitations (section 5.5).

661 

### 5.1 Synthesis of the amplitude of change in erosion rates for model scenarios 1-3

662 The amplitude of change of mean catchment erosion rates [in percentage] varies at a seasonal scale (Fig. 11) between the study  
 663 areas. The amplitude of change in erosion rates to their respective mean values was estimated (Fig. 11) using the coefficient  
 664 of variation in percent (standard deviation divided by the mean of a dataset). The coefficient of variation is a statistical tool to  
 665 compare multiple variables free from scale effects. It is a dimensionless quantity (Brown, 1998). This comparison represents  
 666 the sensitivity of each catchment to changing seasonal weather for all three model scenarios (sections 4.1 – 4.3).  
 667 In scenario 1, with seasonal variations in vegetation cover and constant seasonal precipitation (Fig. 11), the amplitude of  
 668 change in erosion rates ranges between 5% in the arid and 36% in Mediterranean setting. The above results support the findings  
 669 of Zhang et al. (2019), which observed 20–30% of the total change in sediment yield with constant precipitation and variable  
 670 vegetation cover. The above study used the soil and water assessment tool (SWAT) based on NDVI and climate parameters.



671  
 672 **Figure 11.** Stacked bar plot depicting the amplitude of change in seasonal erosion rates (relative to their respective  
 673 means). Scenario 1 is shown in blue and had variable vegetation cover and constant precipitation rates. Scenario 2 is  
 674 shown in orange and had constant vegetation cover and variable precipitation rates, and scenario 3 is shown in green  
 675 and represents the simulation with coupled variations in vegetation cover and precipitation rates.

676 In scenario 2, with constant vegetation cover and variable precipitation rates (Fig. 11), the amplitude of change in erosion rates  
 677 ranges from 13% in the arid setting (AZ) to 52%, 65%, and 91% in humid-temperate (NA), semi-arid (SG) and Mediterranean  
 678 (LC) settings, respectively. A similar trend is observed in scenario 3 with coupled variations in vegetation cover and  
 679 precipitation rates (Fig. 11), with the amplitude of change in erosion rates between 13% in the arid setting up to 50%, 86%,  
 680 and 97% in the humid-temperate, semi-arid and Mediterranean settings, respectively. The magnitude of erosion rate changes  
 681 is amplified in scenario 3, especially in the semi-arid setting (e.g., ~21% increase in the amplitude of change from scenario 2

**Deleted:** a discussion of the effect of variable vegetation and precipitation rates on seasonal erosion rates (section 5.2). Following this, we present

**Deleted:** ).

**Deleted:** 10

**Deleted:** 10

**Deleted:** , i.e., it

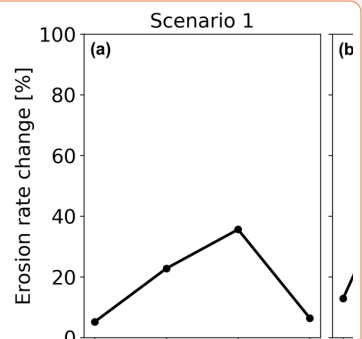
**Deleted:** section

**Deleted:** 10a

**Deleted:** 6.

**Deleted:** humid-temperate setting

**Deleted:** In addition, a 5.5% change in amplitude in erosion rates is observed in the arid setting (Fig. 10a). However, due to the weak correlation between vegetation cover and erosion rates (i.e., Pearson r: 0.17 and p>0.05, Fig. 5) and negligible vegetation cover ( $V < 0.1$ ), it is unclear if these changes in erosion rates are due to changes in vegetation cover alone.



**Deleted:**

**Deleted:** 0

**Deleted:** The

**Deleted:** )

**Deleted:** (a) scenario 1: with

**Deleted:** , (b) scenario

**Deleted:** : with

**Deleted:** (c)

**Deleted:** :

**Deleted:** 10b

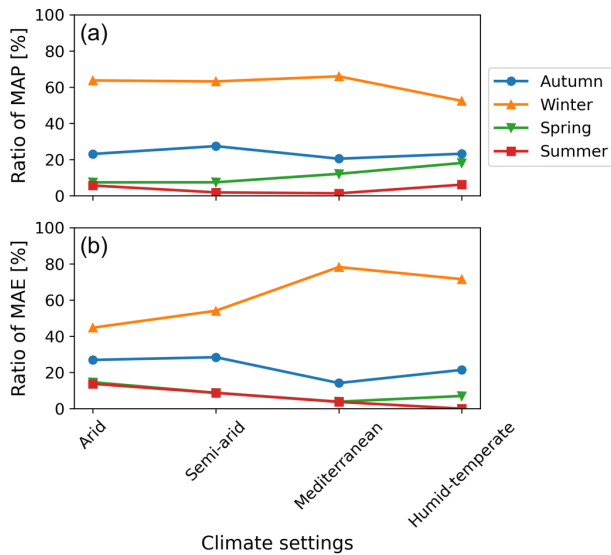
**Deleted:** 10c

710 to scenario 3). This amplification could be owed to the 35% change in vegetation cover in the semi-arid setting (Fig. 8).  
 711 Overall, these observations indicate a high sensitivity of erosion in semi-arid and Mediterranean environments compared to  
 712 arid and humid-temperate settings.

713 The pattern of erosion rate changes in scenarios 1-3 implies a dominant control of precipitation variations (rather than  
 714 vegetation cover change) on catchment erosion rates at a seasonal scale. This interpretation is consistent with previous  
 715 observational studies. For example, a field study by Suescún et al. (2017) in the Columbian Andes highlighted the significant  
 716 influence of precipitation seasonality (over vegetation cover seasonality) on runoff and erosion rates. An observational  
 717 catchment-scale study in the semi-arid Chinese Loess Plateau by Wei et al. (2015) indicated that intra-annual precipitation  
 718 variations were a significant contributor to monthly runoff and sediment yield variations.

## 719 5.2 Synthesis of catchment erosion rates over wet and dry seasons

720 In this section, we discuss the ratio of seasonal precipitation and erosion rates with the mean annual precipitation (MAP) (Fig.  
 721 12a) and mean annual erosion (MAE) (Fig. 12b) during different seasons (i.e., autumn – summer) in a year, averaged over the  
 722 last cycle of the transient simulations (i.e., depicting the erosion rate predictions for 2000 – 2019). These are defined as the  
 723 ratio of the mean erosion (and precipitation) rates in a season (e.g., winter) to the mean annual erosion rates (and MAP) during  
 724 the last 20 years of the transient simulations. This was done to identify the impact of precipitation during wet seasons (in this  
 725 case, winter) in influencing the annual erosion rates. This analysis was performed for the simulation results of scenario 3 for  
 726 different climate and ecological settings (i.e., arid to humid-temperate). We do this specifically with scenario 3 results to  
 727 capture the trends in erosion rates with coupled variations in model input (i.e., precipitation and vegetation cover).



728  
 729 **Figure 12.** The ratio of seasonal precipitation and erosion rates to mean annual precipitation (MAP) and mean annual  
 730 erosion (MAE) during the last cycle of transient simulations results from scenario 3 (coupled seasonal variations in  
 731 precipitation and vegetation cover). The plots correspond to (a) the ratio of MAP per season [%] and (b) ratio of MAE

**Deleted:** predominant

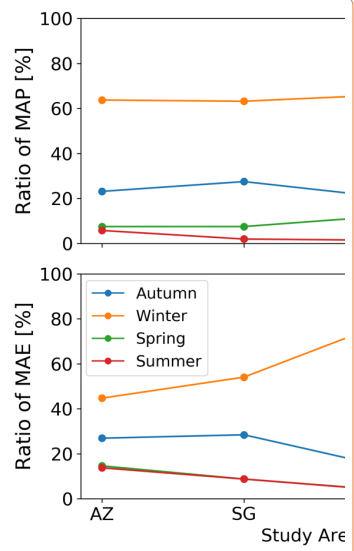
**Deleted:** For example, a plot-scale study by Gabarrón-Galeote et al. (2013) in the Mediterranean environment in Belgium concluded that rainfall intensity was the main factor in determining the observed seasonal soil hydrological and erosive response. Another

**Deleted:** 11a

**Deleted:** 11b

**Deleted:** entire time series

**Deleted:** is



**Deleted:**

**Deleted:** 11

**Deleted:** model variables

**Deleted:** means

**Deleted:** all

**Deleted:** seasons in a year for simulation

748 per season ~~1%~~. Each color and point style represent the ratio for a distinct climate setting i.e., arid, semi-arid  
749 Mediterranean, and humid-temperate settings.

750 The values for the ratio of MAP during different seasons (Fig. ~~12a~~) depicts winter (June-August) and summer (December-  
751 February) as the wettest and driest seasons of the year, respectively. For example, all study areas receive >50% and <6% of  
752 MAP during winters and summers. The same is reflected in Fig. ~~12b~~ with 45%, 55%, 78%, and 71% of MAE in the arid, semi-  
753 arid, Mediterranean, and humid-temperate settings, respectively, during winters. On the contrary, during summers the share of  
754 MAE decreases from 14% in the arid setting to 1% in the humid-temperate setting. The Autumn (March-May) receives lower  
755 precipitation amounts that range from 20–30% of MAP in the study areas. Arid and semi-arid settings experience a relatively  
756 higher share of MAE (e.g., ~30%) than the Mediterranean and humid temperate settings (e.g., ~15–20%). The Spring season  
757 experiences relatively higher erosion rates despite a smaller share of MAP in arid and semi-arid settings. For example, the arid  
758 and semi-arid settings experience 10–14% of the MAE for ~7% of MAP. At the same time, the Mediterranean and humid-  
759 temperate settings experience 5–7% of MAE for ~12–18% of MAP during Spring. Overall, we find that arid and semi-arid  
760 settings experience <15% and ~50% of MAE during the wet (winter) and dry (summer) seasons. The above relationship is  
761 amplified for the Mediterranean and humid-temperate settings with <5% and >70% of MAE occurring during wet and dry  
762 seasons, respectively. The latter is in agreement with an observational study by Mosaffaei et al., (2015) in a Mediterranean  
763 catchment in Iran. More specifically, Mosaffaei et al., (2015) used field observations from 2012–2013 to conclude that  
764 maximum erosion rates (>70%) are observed during the wet season, which decreases in the dry season (<10%).▲

Deleted: [%] of the mean values averaged over the last 20 years of the simulations (2000 - 2019).

Deleted: represents

Deleted: each ecological

Deleted: (Pan de Azúcar, AZ),

Deleted: (Santa Gracia, SG),

Deleted: (La Campana, LC),

Deleted: (Nahuelbuta, NA).

Deleted: 11a

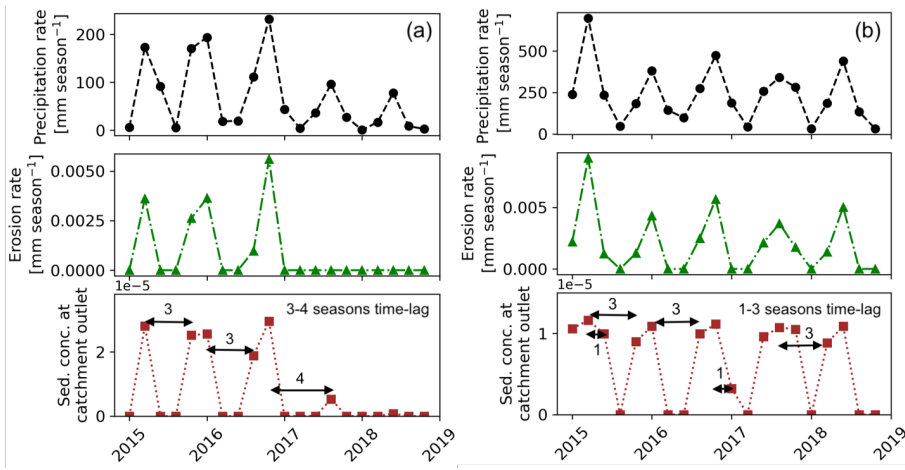
Deleted: 11b

Formatted: Font color: Text 1

Deleted: 5.3

### 765 5.3 Consideration of transient sediment dynamics in model results

766 This section discusses the impact of lag times from when sediment is eroded in a source area until it leaves the catchment  
767 outlet. This analysis was conducted because in natural systems, when sediment is eroded from its source, it takes time to leave  
768 the catchment (in this case the model domain) and recorded as eroded in our analysis. According to field studies and modeling  
769 experiments, this time lag is usually more than a season (3 months) (e.g., Buendia et al., (2016)). To capture these time-lags  
770 in precipitation, erosion and concentration of sediment leaving the catchment outlet, the model output for the Mediterranean  
771 and humid-temperate settings are compared (Fig. 13). We perform this analysis on the simulation results of scenario 3 with  
772 coupled variations in seasonal precipitation and vegetation cover. The concentration of sediment is defined as a dimensionless  
773 quantity ( $Q_s/Q$ ) estimated from sediment flux ( $Q_s$ ) and discharge rates ( $Q$ ).



785  
786 **Figure 13. Simulation results (scenario 3: coupled variations in precipitation in vegetation cover) to capture the time-**  
787 **lags in precipitation, erosion rates and sediment concentration at catchment outlet) over the last five years (Autumn-**  
788 **2015 – Summer-2019) of the last cycle of transient-state model run for the catchments in: (a) Mediterranean and (b)**  
789 **humid-temperate setting.**

790 In the Mediterranean settings, these time lags range from 3 to 4 seasons, and are relatively large (e.g., from wet season 2016  
791 to wet season of 2017, see Fig. 13a). However, in humid-temperate setting, these time lags range from 1 to 3 seasons, mostly  
792 owed to the relatively higher precipitation magnitude and frequency in this region (Fig. 13b). In the catchments in both these  
793 climate settings, the pulse of sediment leaving the catchment is fairly distributed with the maximum concentration of sediment  
794 leaving the catchment in the same wet season when it is eroded from its source. These time-lags would result in enhanced  
795 sensitivity of the proportional changes in erosion rates to the changes in seasonal precipitation and (or) vegetation cover, as  
796 the sediment is transported even in the seasons when the sediment is not eroded from its source (e.g., wet season in 2017 in  
797 both the above climate settings). This poses a limitation to the current study and is again revisited in the model limitations  
798 (section 5.5).

799 **5.4 Comparison to previous studies**

800 In this section, we relate the broad findings of this study to the previously published observational studies. In an observational  
801 study in an agrarian drainage basin in the Belgian Loam Belt, Steegen et al., (2000) evaluated sediment transport over various  
802 time scales (including seasonal). They observed lower sediment fluxes during the seasons with high vegetation cover. In  
803 addition, an observational study by Zheng (2006) investigated the effect of vegetation changes on soil erosion in the Loess  
804 Plateau, China, and concluded that soil erosion was significantly reduced (up to ~50%) after vegetation restoration. Another  
805 observational study in semi-arid grasslands in the Loess Plateau, China, by Hou et al., (2020) highlighted a considerable  
806 reduction in erosion rates due to the development of richness and evenness of the plant community in the early to the mid wet  
807 season. Our results from scenario 1 (seasonal variations in vegetation cover with constant precipitation rates) support the  
808 findings of the above studies whereby a negative correlation (Kendall τ: -0.4 to -0.5) was found between vegetation cover and  
809 erosion rates in humid-temperate and Mediterranean settings (see Fig. 5).

**Deleted:** Pearson r: ~ –

**Deleted:** 6 and p <

**Deleted:** 05

**Deleted:** for the semi-arid

**Deleted:** . More specifically, we found erosion rates decrease with an increase in vegetation cover in Santa Gracia (semi-arid) and La Campana (Mediterranean) (see Fig. 5). However, a positive correlation (Pearson r: ~0.3 and p<0.05) is observed in the humid-temperate setting from dry season to wet season

820 A catchment-scale observational study in Baspa Valley, NW Himalayas (Wulf et al., 2010), analyzed seasonal precipitation  
821 gradients and their impact on fluvial erosion using weather station observations (1998 – 2007). The study observed a positive  
822 correlation between precipitation and sediment yield variability, demonstrating the summer monsoon's first-order control on  
823 erosion processes. An observational study by Wei et al., (2015) in Loess Plateau, China, evaluated erosion and sediment  
824 transport under various vegetation types and precipitation variations. They found that significant changes in landscape pattern  
825 and vegetation coverage (i.e., land use land cover) might contribute to long-term dynamics of soil loss. However, seasonal  
826 variations in runoff and sediment yield were mainly influenced by rainfall seasonality. In comparison to the results of this  
827 study, we find the similarity in the patterns of erosion rates in scenario 2 (variable precipitation and constant vegetation cover)  
828 and scenario 3 (coupled variations in precipitation and vegetation) are consistent with the findings of Wei et al., (2015). For  
829 example, the amplitude of change in erosion rates (Fig. 10) in scenarios 2 and 3 differ by 0%, 6%, and -2% in the arid,  
830 Mediterranean, and humid-temperate settings, respectively. However, this difference is enhanced in the semi-arid region (i.e.,  
831 ~23%) due to a relatively high degree of variation (~25%) in seasonal vegetation cover change.

832 Finally, an observational study in the Columbian Andes by Suescún et al., (2017) assessed the impact of seasonality on  
833 vegetation cover and precipitation and found higher erosion rates in regions with steeper slopes. Another study by Chakrapani  
834 (2005) emphasized the direct impact of local relief and channel slope on sediment yield in natural rivers. The broad findings  
835 of the above studies agree with our results from scenarios 1-3, as we find higher erosion rates in the Mediterranean and humid-  
836 temperate regions with steeper topography (mean slope ~20 deg), which encounter high seasonality (and intensity) in  
837 precipitation.

### 838 5. Model Limitations

839 The model setup used in this study was designed to quantify the sensitivity of erosion rates in different climate and ecological  
840 settings with variations in precipitation rates and vegetation cover at seasonal scales. We represent the degree of variations in  
841 erosion rates in terms of changes in the amplitude (with respect to the mean) for different model scenarios (see sections 4.1 –  
842 4.3).

843 Our modeling approach used several simplifying assumptions that warrant discussion and are avenues for investigation in  
844 future studies. For example, model results presented here successfully capture the major surface processes, including  
845 vegetation-dependent erosion and infiltration, sediment transport, and surface runoff. However, groundwater flow is not  
846 considered in the current study, and how the reentry of groundwater into streams over seasonal scales would influence  
847 downstream erosion. The reason is that groundwater flow modeling includes a high amount of heterogeneity and anisotropy  
848 and requires much finer grid sizes (<1m) and smaller time steps (in seconds to hours). Thus, due to the large grid-cell size (90  
849 m), timescales (monthly), and high uncertainty in subsurface hydrologic parameters we were unable to evaluate the effects of  
850 groundwater flow on our results. Furthermore, this study assumed uniform lithologic and hydrologic parameters (e.g., vertical  
851 hydraulic conductivity, initial soil moisture, evapotranspiration, erodibility, etc.) over the entire catchment. As said earlier,  
852 these properties are subject to a high level of uncertainty and heterogeneity, the best fitting parameters, based on previously  
853 published literature (e.g., Schaller et al., 2018; Bernhard et al., 2018; Schmid et al., 2018; Sharma et al., 2021) are used for the  
854 model simulations. However, the heterogeneity in vegetation cover and related soil-water infiltration per grid cell is used in  
855 this study. For the heterogeneity in vegetation cover, we use MODIS-derived NDVI as a proxy of vegetation cover. According  
856 to Garatuza-Payán et al. (2005), NDVI is assumed as an effective tool for estimating seasonal changes in vegetation cover  
857 density. However, the spatial resolution (250 m) of the NDVI dataset is lower than that of the SRTM DEM (90 m) used in the  
858 study. Nevertheless, the difference in spatial resolution of vegetation cover and topography might introduce ambiguity in the  
859 model results. Furthermore, transient dynamics associated with sediment storage in the model is not incorporated in the study  
860 to capture the time lag required for the eroded sediment to move out of the model domain. As the LFM (SPACE 1.0) used in

**Deleted:** soil

**Deleted:** 4

**Deleted:** We represent the degree of variations in erosion rates in terms of change amplitude (with respect to the mean) for different model scenarios (see sections 4.1 – 4.3). This study was intended to introduce temporal downscaling (from millennial to seasonal time scales) to the approach of previous similar modeling studies (e.g., Schmid et al., 2018; Sharma et al., 2021).

**Deleted:** potential

**Deleted:** lithological

**Deleted:** hydrological

**Deleted:** subjected

874 this study shuffles between detachment- and transport-limited fluvial erosion, we suspect that in such short timescales (3  
875 months) and in small catchments, detachment-limited fluvial erosion is dominant. Hence, any sediment removed from its  
876 source is transported out of the domain in a given time-step. However, it is recommended for future studies considering larger  
877 or lower gradient catchments, where sediment storage may be more significant than documented here, an analysis of erosion  
878 at a local scale (e.g., at individual model grid cells) is recommended.

879 A final limitation stems from several generalized model parameters (e.g., rock uplift rate, erodibility, diffusivity, etc.) applied  
880 to the SRTM DEM (as initial topography). We did this to capture the effects of seasonality in precipitation and vegetation  
881 cover in modern times (2000 - 2019). However, the current topography might not have evolved with the same tectonic and  
882 lithological parameters. To address this limitation, we conducted simulations for 50 iterations and detrended the model results  
883 to remove those transient effects (see section 3.6). This limitation can be handled in future studies by parameterizing the model  
884 to the current topography using stochastic (e.g., Bayesian) techniques (e.g., Stephenson et al., 2006; Avdeev et al., 2011). As  
885 this study was aimed to capture the control of seasonal precipitation and (or) vegetation changes on the relative variability of  
886 erosion rates, the above limitation may not pose a problem in the model results.

**Deleted:** simulated the model

## 887 6 Summary and Conclusions

888 In this study, we applied a landscape evolution model to quantify the impact of seasonal variations in precipitation and  
889 vegetation on catchment averaged erosion rates. We performed this in regions with varied climate and ecology including: arid,  
890 semi-arid, Mediterranean, and humid-temperate settings. Three sets of simulations were designed to model erosion rates for  
891 (a) scenario 1: constant precipitation and variable vegetation cover, (b) scenario 2: variable precipitation and constant  
892 vegetation cover, and (c) scenario 3: coupled variations in precipitation and vegetation cover. The main conclusions derived  
893 from this study are as follows:

- 894 1. Scenario 1, with variable vegetation cover and constant precipitation (Fig. 4), resulted in small variations in seasonal  
895 erosion rates ( $<0.02 \text{ mm yr}^{-1}$ ) in comparison to the other scenarios. The amplitude of change in seasonal erosion rates  
896 (relative to the mean) is the smallest in humid-temperate setting and maximum in the Mediterranean setting (Fig.  
897 10a). For example, it ranges from 5% in the arid setting (Pan de Azúcar) to 23% and 36% in the semi-arid (Santa  
898 Gracia) and Mediterranean settings (La Campana), respectively.
- 899 2. Scenario 2, with constant vegetation cover and variable precipitation (Fig. 6), results in relatively higher seasonal  
900 erosion rates ( $<0.06 \text{ mm yr}^{-1}$ ) in comparison to scenario 1. The amplitude of change in seasonal erosion rates (relative  
901 to the mean) is smallest in the arid setting and largest in the Mediterranean setting (Fig. 10b). For example, it ranges  
902 from 13% in the arid setting (Pan de Azúcar) to 52%, 65%, and 91% in the humid-temperate (Nahuelbuta), semi-arid  
903 (Santa Gracia), and Mediterranean settings (La Campana), respectively.
- 904 3. Scenario 3, with coupled variations in vegetation cover and precipitation (Fig. 8), results in similar seasonal erosion  
905 rates ( $<0.06 \text{ mm yr}^{-1}$ ) to scenario 2. Similarly, the amplitude of change in seasonal erosion rates (relative to the mean)  
906 is the smallest in the arid setting and the largest in the Mediterranean setting (Fig. 10c). For example, it ranges from  
907 13% in the arid setting (Pan de Azúcar) to 50%, 86%, and 97% in the humid-temperate (Nahuelbuta), semi-arid (Santa  
908 Gracia), and Mediterranean settings (La Campana), respectively. A significant increase (from scenario 2) in the  
909 variation in erosion rates (~21%) is owed to the ~25% variation in vegetation cover in semi-arid settings.
- 910 4. All study areas experience maximum and minimum erosion during wet and dry seasons, respectively (Fig. 11b).  
911 However, the difference (in maximum and minimum) is amplified from the arid (~30%) to the Mediterranean and  
912 humid-temperate settings (~70-75%). This is owed to the range of amplitude of precipitation rate change (Fig. 7)  
913 increasing from the arid (e.g., ~9 mm) to humid-temperate settings (e.g., ~543 mm) in wet and dry seasons.

**Deleted:** 6.

**Deleted:** humid-temperate

**Deleted:** Nahuelbuta

**Deleted:** the

919 Finally, this study was motivated by testing the hypotheses that (1) if precipitation variations primarily influence seasonal  
 920 erosion, then the influence of seasonal vegetation cover changes would be less significant, and (2) catchment erosion in drier  
 921 settings is more sensitive to seasonality in precipitation and vegetation, than wetter settings. With respect to hypothesis 1, we  
 922 found that seasonal precipitation variations primarily drive catchment erosion and the effects of vegetation cover variations  
 923 are secondary. Results presented here (Fig. 10b) support this interpretation with ~~a~~ high amplitude of change in erosion rates  
 924 (with respect to means) ranging from 13 to 91% for the scenario with constant vegetation cover and seasonal precipitation  
 925 variations. However, the effect of seasonal vegetation cover changes is also significant (Fig. 10a), ranging between 5 – 36%.  
 926 Hence, the first hypothesis is partially confirmed, but the magnitude of response depends on the ecological zone investigated.  
 927 Concerning hypothesis 2, we found that seasonal changes in catchment erosion are more pronounced in the semi-arid and  
 928 Mediterranean settings and less pronounced in the arid and humid temperate settings. This interpretation is supported by Fig.  
 929 10c, with a significantly high amplitude of change in catchment erosion in semi-arid (~86%) and Mediterranean (~97%)  
 930 settings with relatively lower changes in humid temperate (~50%) and arid (~13%) settings, partially confirming the  
 931 hypothesis.

**Deleted:** significantly

**Deleted:** )

### 932 Appendix A: Input parameters with corresponding units for the landscape evolution model

933 **Table A1. Input parameters with corresponding units for the landscape evolution model**

<b>Model Parameters</b>	<b>Values</b>	<b>Model Parameters</b>
Grid spacing (dx)	90 m	Grid spacing (dx)
Model runtime (totalT)	1000 years (2000 - 2019 repeated over 50 times)	Model runtime (totalT)
time-step (dt)	1 season (3 months)	time-step (dt)
Rock uplift rate (U) <sup>1</sup>	$1.25 \times 10^{-5}$ [m season <sup>-1</sup> ] (or 0.05 [mm a <sup>-1</sup> ])	Rock uplift rate (U) <sup>1</sup>
Initial sediment thickness (H_initial) <sup>2</sup>	20 (A*), 45 (SA*), 60 (M*), 70 (HT*) [cm]	Initial sediment thickness (H_initial) <sup>2</sup>
Bedrock erodibility (Kr) <sup>1</sup>	$2 \times 10^{-9}$ [m <sup>-1</sup> ]	Bedrock erodibility (Kr) <sup>1</sup>
Sediment erodibility (Ks) <sup>1</sup>	$2 \times 10^{-8}$ [m <sup>-1</sup> ]	Sediment erodibility (Ks) <sup>1</sup>
Reach scale bedrock roughness (H*) <sup>1</sup>	1 [m]	Reach scale bedrock roughness (H*) <sup>1</sup>
Porosity ( $\phi$ ) <sup>4</sup>	0.51 (A*), 0.43 (SA*), 0.51 (M*), 0.7 (HT*) [-]	Porosity ( $\phi$ ) <sup>4</sup>
Fraction of fine sediments (Ff) <sup>1</sup>	0.2 [-]	Fraction of fine sediments (Ff) <sup>1</sup>
Effective terminal settling velocity (Vs) <sup>1</sup>	2.5 [mm season <sup>-1</sup> ]	Effective terminal settling velocity (Vs) <sup>1</sup>
m, n <sup>1</sup>	0.6, 1 [-]	m, n <sup>1</sup>
Bedrock erosion threshold stream power ( $\omega_{cr}$ ) <sup>1</sup>	$1.25 \times 10^{-5}$ [m season <sup>-1</sup> ]	Bedrock erosion threshold stream power ( $\omega_{cr}$ ) <sup>1</sup>
Sed. entr. threshold stream power ( $\omega_{cs}$ ) <sup>1</sup>	$1.25 \times 10^{-6}$ [m season <sup>-1</sup> ]	Sed. entr. threshold stream power ( $\omega_{cs}$ ) <sup>1</sup>
Bare soil diffusivity ( $K_b$ ) <sup>1</sup>	$2.5 \times 10^{-4}$ [m <sup>2</sup> season <sup>-1</sup> ]	Bare soil diffusivity ( $K_b$ ) <sup>1</sup>
Exponential decay coefficient ( $\alpha$ ) <sup>1</sup>	0.3 [-]	Exponential decay coefficient ( $\alpha$ ) <sup>1</sup>
Critical channel formation area ( $A_{crit}$ ) <sup>3</sup>	$1 \times 10^6$ [m <sup>2</sup> ]	Critical channel formation area ( $A_{crit}$ ) <sup>3</sup>
Reference vegetation cover ( $V_r$ ) <sup>3</sup>	1 (100%)	Reference vegetation cover ( $V_r$ ) <sup>3</sup>
Manning's number for bare soil ( $n_s$ ) <sup>3</sup>	0.01 [-]	Manning's number for bare soil ( $n_s$ ) <sup>3</sup>
Manning's number for ref. vegetation ( $n_v$ ) <sup>3</sup>	0.6 [-]	Manning's number for ref. vegetation ( $n_v$ ) <sup>3</sup>
Scaling factor for vegetation influence (w) <sup>3</sup>	1 [-]	Scaling factor for vegetation influence (w) <sup>3</sup>
Soil bulk density (B) <sup>4</sup>	1300 (A*), 1500 (SA*), 1300 (M*), 800 (HT*) [kg m <sup>-3</sup> ]	Soil bulk density (B) <sup>4</sup>
Soil type <sup>4</sup>	sandy loam (A*, SA*, and M*); sandy clay loam (HT*)	Soil type <sup>4</sup>
Initial soil moisture (s) <sup>5</sup>	0.058 (A*), 0.02 (SA*), 0.053 (M*), 0.15 (HT*) [m <sup>3</sup> m <sup>-3</sup> ]	Initial soil moisture (s) <sup>4</sup>

**Deleted:**

<sup>1</sup>Sharma<sup>¶</sup>

935 <sup>1</sup>Sharma et al. (2021), <sup>2</sup>Schaller et al. (2018), <sup>3</sup>Schmid et al. (2018), <sup>4</sup>Bernhard et al. (2018), <sup>5</sup>Übernickel et al. (2020).

940 \*A: arid; SA: semi-arid; M: Mediterranean; HT: humid-temperate setting.

941

#### 942 Appendix B: Implementation of vegetation dependent hillslope and Fluvial processes in Landlab components

943 This section includes the description of vegetation dependent hillslope and fluvial processes defined in the Landlab components  
944 used in this study, based on the approaches by Istanbulluoglu (2005) Schmid et al., (2018), and Sharma et al., (2021).

##### 945 B1 Vegetation dependent hillslope processes

946 The rate of change in topography due to hillslope diffusion (Fernandes and Dietrich, 1997) is defined as follows:

947 
$$\frac{\partial z}{\partial t} (\text{hillslope}) = \nabla q_s, \quad (\text{A1})$$

948 where  $q_s$  is sediment flux along the slope  $S$ . We applied slope and depth-dependent linear diffusion rule following the approach  
949 of Johnstone and Hilley (2014) such that:

950 
$$q_s = K_d S d_* (1 - e^{-H/d_*}), \quad (\text{A2})$$

951 where  $K_d$  is diffusion coefficient [ $\text{m}^2 \text{ yr}^{-1}$ ],  $d_*$  is sediment transport decay depth [m], and  $H$  denotes sediment thickness.

952 The diffusion coefficient is defined as a function of vegetation cover present on hillslopes, which is estimated following the  
953 approach of Istanbulluoglu (2005), as follows:

954 
$$K_d = K_b e^{-(\alpha V)}, \quad (\text{A3})$$

955 where  $K_b$  is defined as a function of vegetation cover  $V$ , an exponential decay coefficient  $\alpha$ , and linear diffusivity  $K_b$  for bare  
956 soil.

##### 957 B2 Vegetation dependent fluvial processes

958 The fluvial erosion is estimated for a two-layer topography (i.e., bedrock and sediment are treated explicitly) in the coupled  
959 detachment- / transport-limited model, SPACE 1.0 (Shobe et al., 2017). Bedrock erosion and sediment entrainment are  
960 calculated simultaneously in the model. Total fluvial erosion is defined as:

961 
$$\frac{\partial z}{\partial t} (\text{fluvial}) = \frac{\partial R}{\partial t} + \frac{\partial H}{\partial t}, \quad (\text{A4})$$

962 where, left-hand side denotes the total fluvial erosion rate. The first and second terms on right-hand side denote the bedrock  
963 erosion rate and sediment entrainment rate.

964 The rate of change of height of bedrock  $R$  per unit time [ $\text{m yr}^{-1}$ ] is defined as:

965 
$$\frac{\partial R}{\partial t} = U - E_r, \quad (\text{A5})$$

966 where  $E_r$  [ $\text{m yr}^{-1}$ ], is the volumetric erosion flux of bedrock per unit bed area.

967 The change in sediment thickness  $H$  [m] per unit time [yr] is defined as a fraction net deposition rate and solid fraction  
968 sediments, as follows:

969 
$$\frac{\partial H}{\partial t} = \frac{D_s - E_s}{1 - \phi}, \quad (\text{A6})$$

970 where,  $D_s$  [ $\text{m yr}^{-1}$ ] is the deposition flux of sediment,  $E_s$  [ $\text{m yr}^{-1}$ ] is volumetric sediment entrainment flux per unit bed area, and  
971  $\phi$  is the sediment porosity.

972 Following the approach of Shobe et al. (2017),  $E_s$  and  $E_r$  given by:

$$973 E_s = (K_s q^m S^n - \omega_{cs}) \left(1 - e^{-\frac{H}{H_*}}\right), \quad (A7)$$

$$974 E_r = (K_r q^m S^n - \omega_{cr}) e^{-H/H_*}, \quad (A8)$$

975 where,  $K_s$  [ $\text{m}^{-1}$ ] and  $K_r$  [ $\text{m}^{-1}$ ] are the sediment erodibility and bedrock erodibility parameters respectively. The threshold stream  
976 power for sediment entrainment and bedrock erosion are denoted as  $\omega_{cs}$  [ $\text{m yr}^{-1}$ ] and  $\omega_{cr}$  [ $\text{m yr}^{-1}$ ] in above equations. Bedrock  
977 roughness is denoted as  $H_*$  [m] and the term  $e^{-H/H_*}$  corresponds to the soil production from bedrock. With higher bedrock  
978 magnitudes, more sediment would be produced.

979  $K_s$  and  $K_r$  were modified in the model runtime scripts by introducing the effect of Manning's roughness to quantify the effect  
980 of vegetation cover on bed shear stress in each model cell:

$$981 \tau_v = \rho_w g (n_s + n_v)^{6/10} q^m S^n F_t, \quad (A9)$$

982 where,  $\rho_w$  [ $\text{kg m}^{-3}$ ] and  $g$  [ $\text{m s}^{-2}$ ] are the density of water and acceleration due to gravity respectively. Manning's numbers for  
983 bare soil and vegetated surface are denoted as  $n_s$  and  $n_v$ .  $F_t$  represents shear stress partitioning ratio. Manning's number for  
984 vegetation cover and  $F_t$  are calculated as follows:

$$985 n_v = n_{vr} \left(\frac{V}{V_r}\right)^w \quad (A10)$$

$$986 F_t = \left(\frac{n_s}{n_s + n_v}\right)^{\frac{3}{2}} \quad (A11)$$

987 where,  $n_{vr}$  is Manning's number for the reference vegetation. Here,  $V_r$  is reference vegetation cover ( $V = 100\%$ ) and  $V$  is local  
988 vegetation cover in a model cell,  $w$  is empirical scaling factor.

989 By combining stream power equation (Tucker et al., 1999; Howard, 1994; Whipple and Tucker, 1999) and above concept of  
990 the effect of vegetation on shear stress, we follow the approach of Schmid et al. (2018) and Sharma et al. (2021) to define new  
991 sediment and bedrock erodibility parameters influenced by the surface vegetation cover on fluvial erosion, as follows:

$$992 K_{vs} = K_s \rho_w g (n_s + n_v)^{6/10} F_t, \quad (A12)$$

$$993 K_{vr} = K_r \rho_w g (n_s + n_v)^{6/10} F_t, \quad (A13)$$

994 where,  $K_{vs}$  [ $\text{m}^{-1}$ ] and  $K_{vr}$  [ $\text{m}^{-1}$ ] are modified sediment erodibility and bedrock erodibility respectively. These are influenced by  
995 the effect of presence of fraction of vegetation cover  $V$ . Hence,  $K_s$  and  $K_r$  in Eq. (8) and Eq. (9) are replaced by  $K_{vs}$  and  $K_{vr}$  to  
996 include an effect of vegetation cover on fluvial processes in the model. The trends of  $K_d$ ,  $K_{vs}$  and  $K_{vr}$  are illustrated in Fig. 3  
997 in Sharma et al., (2021).

998 **Code and data availability**

999 The code and data used in this study are freely available via Zenodo (<https://doi.org/10.5281/zenodo.8033782>, Sharma and  
000 Ehlers, 2023).

**Deleted:** The code and data used in this study are freely available upon request. 

001 **Author contributions**

002 HS and TAE designed the initial model setup and simulation programs. HS and TAE conducted model modifications,  
003 simulation runs, and analysis. HS prepared the paper with contributions from TAE.

006 **Competing interests**

007 The authors declare that they have no conflict of interest.

008 **Acknowledgments**

009 We acknowledge the support from the Open Access Publishing fund of the University of Tübingen. We would like to thank  
010 two anonymous reviewers and Omer Yetemen for their constructive reviews. We also thank Simon Mudd for editing this  
011 paper.

**Deleted:** Hemanti Sharma and Todd A. Ehlers  
**Deleted:** Fund  
**Deleted:** acknowledge

012 **Financial support**

013 This research has been supported by the Deutsche Forschungsgemeinschaft (grant nos. EH329/14-2, SPP-1803, and Research  
014 Training Group 1829 Integrated Hydrosystem Modelling).

**Formatted:** Font: Bold, Font color: Auto  
**Deleted:** from the  
**Formatted:** Font color: Auto,  
**Deleted:**  
**Formatted:** Font color: Auto,  
**Deleted:**, funded by the German Research Foundation (DFG). In addition, Todd A. Ehlers acknowledges support from the German priority research program "EarthShape: Earth Surface Shaping  
**Formatted:** Font color: Auto,  
**Deleted:** Biota" (SPP-1803; EH329/14-2). We thank xxx and yy for their constructive reviews  
**Formatted:** Font color: Auto,  
**Formatted:**

015 **Review Statement**

016 This paper was edited by Simon Mudd and reviewed by two anonymous reviewers and Omer Yetemen.

017 **References**

- 018 Avdeev, B., Niemi, N. A., and Clark, M. K.: Doing more with less: Bayesian estimation of erosion models with detrital  
019 thermochronometric data, *Earth Planet. Sci. Lett.*, 305, 385–395, <https://doi.org/10.1016/j.epsl.2011.03.020>, 2011.
- 020 Barnhart, K. R., Glade, R. C., Shobe, C. M., and Tucker, G. E.: Terrainbento 1.0: a Python package for multi-model analysis  
021 in long-term drainage basin evolution, *Geosci. Model Dev.*, 12, 1267–1297, <https://doi.org/10.5194/gmd-12-1267-2019>, 2019.
- 022 Beaudoin, H., Rodell, M., and NASA/GSFC/HSL: GLDAS Noah Land Surface Model L4 monthly 0.25 x 0.25 degree,  
023 Version 2.1, <https://doi.org/10.5067/SXAVCZFAQLNO>, 2020.
- 024 Bernhard, N., Moskwa, L.-M., Schmidt, K., Oeser, R. A., Aburto, F., Bader, M. Y., Baumann, K., von Blanckenburg, F., Boy,  
025 J., van den Brink, L., Brucker, E., Büdel, B., Canessa, R., Dippold, M. A., Ehlers, T. A., Fuentes, J. P., Godoy, R., Jung, P.,  
026 Karsten, U., Köster, M., Kuzyakov, Y., Leinweber, P., Neidhardt, H., Matus, F., Mueller, C. W., Oelmann, Y., Oses, R., Osse,  
027 P., Paulino, L., Samolov, E., Schaller, M., Schmid, M., Spielvogel, S., Spohn, M., Stock, S., Stroncik, N., Tielbörger, K.,  
028 Übernickel, K., Scholten, T., Seguel, O., Wagner, D., and Kühn, P.: Pedogenic and microbial interrelations to regional climate  
029 and local topography: New insights from a climate gradient (arid to humid) along the Coastal Cordillera of Chile, *CATENA*,  
030 170, 335–355, <https://doi.org/10.1016/j.catena.2018.06.018>, 2018.
- 031 Bookhagen, B., Thiede, R. C., and Strecker, M. R.: Abnormal monsoon years and their control on erosion and sediment flux  
032 in the high, arid northwest Himalaya, *Earth Planet. Sci. Lett.*, 231, 131–146, <https://doi.org/10.1016/j.epsl.2004.11.014>, 2005.
- 033 Brown, C. E.: Coefficient of Variation, in: *Applied Multivariate Statistics in Geohydrology and Related Sciences*, Springer,  
034 Berlin, Heidelberg, 1998.
- 035 Buendia, C., Vericat, D., Batalla, R. J., and Gibbins, C. N.: Temporal Dynamics of Sediment Transport and Transient In-  
036 channel Storage in a Highly Erodible Catchment: LINKING SEDIMENT SOURCES, RAINFALL PATTERNS AND  
037 SEDIMENT YIELD, *Land Degrad. Dev.*, 27, 1045–1063, <https://doi.org/10.1002/ldr.2348>, 2016.
- 038 Carretier, S., Tolorza, V., Regard, V., Aguilar, G., Bermúdez, M. A., Martinod, J., Guyot, J.-L., Hérail, G., and Riquelme, R.:  
039 Review of erosion dynamics along the major N-S climatic gradient in Chile and perspectives, *Geomorphology*, 300, 45–68,  
040 <https://doi.org/10.1016/j.geomorph.2017.10.016>, 2018.
- 041 Cerdà, A.: The influence of aspect and vegetation on seasonal changes in erosion under rainfall simulation on a clay soil in  
042 Spain, *Can. J. Soil Sci.*, 78, 321–330, <https://doi.org/10.4141/S97-060>, 1998.

- 054 Chakrapani, G. J.: Factors controlling variations in river sediment loads, *Curr. Sci.*, 88, 569–575, 2005.
- 055 Deal, E., Favre, A. C., and Braun, J.: Rainfall variability in the Himalayan orogen and its relevance to erosion processes: RAINFALL VARIABILITY IN THE HIMALAYAS, *Water Resour. Res.*, 53, 4004–4021, https://doi.org/10.1002/2016WR020030, 2017.
- 058 Didan, Kamel: MOD13Q1 MODIS/Terra Vegetation Indices 16-Day L3 Global 250m SIN Grid V006, https://doi.org/10.5067/MODIS/MOD13Q1.006, 2015.
- 060 Earth Resources Observation And Science (EROS) Center: Shuttle Radar Topography Mission (SRTM) Void Filled, https://doi.org/10.5066/F7F76B1X, 2017.
- 062 Fernandes, N. F. and Dietrich, W. E.: [Hillslope evolution by diffusive processes: The timescale for equilibrium adjustments](#), *Water Resour. Res.*, 33, 1307–1318, https://doi.org/10.1029/97wr00534, 1997.
- 064 Ferreira, V. and Panagopoulos, T.: Seasonality of Soil Erosion Under Mediterranean Conditions at the Alqueva Dam Watershed, *Environ. Manage.*, 54, 67–83, https://doi.org/10.1007/s00267-014-0281-3, 2014.
- 066 Gabarrón-Galeote, M. A., Martínez-Murillo, J. F., Quesada, M. A., and Ruiz-Sinoga, J. D.: Seasonal changes in the soil hydrological and erosive response depending on aspect, vegetation type and soil water repellency in different Mediterranean microenvironments, *Solid Earth*, 4, 497–509, https://doi.org/10.5194/se-4-497-2013, 2013.
- 069 Gao, P., Li, Z., and Yang, H.: Variable discharges control composite bank erosion in Zoige meandering rivers, *CATENA*, 204, 105384, https://doi.org/10.1016/j.catena.2021.105384, 2021.
- 071 Garatuza-Payán, J., Sánchez-Andrés, R., Sánchez-Carrillo, S., and Navarro, J. M.: Using remote sensing to investigate erosion rate variability in a semiarid watershed, due to changes in vegetation cover, *IAHS Publ.*, 292, 144–151, 2005.
- 073 Glodny, J., Gräfe, K., Echtler, H., and Rosenau, M.: Mesozoic to Quaternary continental margin dynamics in South-Central Chile (36–42°S): the apatite and zircon fission track perspective, *Int. J. Earth Sci.*, 97, 1271–1291, https://doi.org/10.1007/s00531-007-0203-1, 2008.
- 076 Green, W. H. and Ampt, G. A.: Studies on Soil Phyics., *J. Agric. Sci.*, 4, 1–24, https://doi.org/10.1017/S0021859600001441, 1911.
- 078 Hancock, G. and Lowry, J.: Hillslope erosion measurement—a simple approach to a complex process, *Hydrol. Process.*, 29, 4809–4816, 2015.
- 080 Hancock, G. and Lowry, J.: Quantifying the influence of rainfall, vegetation and animals on soil erosion and hillslope connectivity in the monsoonal tropics of northern Australia, *Earth Surf. Process. Landf.*, 46, 2110–2123, https://doi.org/10.1002/esp.5147, 2021.
- 083 Herrmann, S. M. and Mohr, K. I.: A Continental-Scale Classification of Rainfall Seasonality Regimes in Africa Based on Gridded Precipitation and Land Surface Temperature Products, *J. Appl. Meteorol. Climatol.*, 50, 2504–2513, https://doi.org/10.1175/JAMC-D-11-024.1, 2011.
- 086 Hobley, D. E. J., Adams, J. M., Nudurupati, S. S., Hutton, E. W. H., Gasparini, N. M., Istanbulluoglu, E., and Tucker, G. E.: Creative computing with Landlab: an open-source toolkit for building, coupling, and exploring two-dimensional numerical models of Earth-surface dynamics, *Earth Surf. Dyn.*, 5, 21–46, https://doi.org/10.5194/esurf-5-21-2017, 2017.
- 089 Hou, J., Zhu, H., Fu, B., Lu, Y., and Zhou, J.: Functional traits explain seasonal variation effects of plant communities on soil erosion in semiarid grasslands in the Loess Plateau of China, *Catena*, v. 194, 104743-, https://doi.org/10.1016/j.catena.2020.104743, 2020.
- 092 Howard, A. D.: [A detachment-limited model of drainage basin evolution](#), *Water Resour. Res.* V 30, 2261–2285, 1994.
- 093 Huete, A., Didan, K., Miura, T., Rodriguez, E. P., Gao, X., and Ferreira, L. G.: [Overview of the radiometric and biophysical performance of the MODIS vegetation indices](#), *Remote Sens. Environ.*, 83, 195–213, https://doi.org/10.1016/S0034-4257(02)00096-2, 2002.
- 096 Istanbulluoglu, E.: [Vegetation-modulated landscape evolution: Effects of vegetation on landscape processes, drainage density, and topography](#), *J. Geophys. Res.*, 110, https://doi.org/10.1029/2004jf000249, 2005.

- .098 Istanbulluoglu, E. and Bras, R. L.: On the dynamics of soil moisture, vegetation, and erosion: Implications of climate variability  
.099 and change, *Water Resour. Res.*, 42, 2006.
- .100 Johnstone, S. A. and Hillyer, G. E.: Lithologic control on the form of soil-mantled hillslopes, *Geology*, 43, 83–86,  
.101 https://doi.org/10.1130/G36052.1, 2014.
- .102 Julien, P. Y., Saghafian, B., and Ogden, F. L.: RASTER-BASED HYDROLOGIC MODELING OF SPATIALLY-VARIED  
.103 SURFACE RUNOFF1, *JAWRA J. Am. Water Resour. Assoc.*, 31, 523–536, https://doi.org/10.1111/j.1752-  
.104 1688.1995.tb04039.x, 1995.
- .105 Langbein, W. B. and Schumm, S. A.: Yield of sediment in relation to mean annual precipitation, *Eos Trans. Am. Geophys.  
.106 Union*, 39, 1076–1084, https://doi.org/10.1029/TR039i006p01076, 1958.
- .107 Leyland, J., Hackney, C. R., Darby, S. E., Parsons, D. R., Best, J. L., Nicholas, A. P., Aalto, R., and Lague, D.: Extreme flood-  
.108 driven fluvial bank erosion and sediment loads: direct process measurements using integrated Mobile Laser Scanning (MLS)  
.109 and hydro-acoustic techniques: Direct measurement of flood-driven erosion using MLS and MBES, *Earth Surf. Process.  
.110 Landf.*, 42, 334–346, https://doi.org/10.1002/esp.4078, 2016.
- .111 Melnick, D.: Rise of the central Andean coast by earthquakes straddling the Moho, *Nat. Geosci.*, 9, 401–407,  
.112 https://doi.org/10.1038/ngeo2683, 2016.
- .113 Melnick, D., Bookhagen, B., Strecker, M. R., and Echtler, H. P.: Segmentation of megathrust rupture zones from fore-arc  
.114 deformation patterns over hundreds to millions of years, Arauco peninsula, Chile: EARTHQUAKE SEGMENTATION AT  
.115 ARAUCO, *J. Geophys. Res. Solid Earth*, 114, https://doi.org/10.1029/2008JB005788, 2009.
- .116 Mosaffaie, J., Ekhtesasi, M. R., Dastorani, M. T., Azimzadeh, H. R., and Zare Chahuki, M. A.: Temporal and spatial variations  
.117 of the water erosion rate, *Arab. J. Geosci.*, 8, 5971–5979, https://doi.org/10.1007/s12517-014-1628-z, 2015.
- .118 Oeser, R. A., Stroncik, N., Moskwa, L.-M., Bernhard, N., Schaller, M., Canessa, R., Brink, L. van den, Köster, M., Brucker,  
.119 E., Stock, S., Fuentes, J. P., Godoy, R., Matus, F. J., Pedraza, R. O., McIntyre, P. O., Paulino, L., Seguel, O., Bader, M. Y.,  
.120 Boy, J., Dippold, M. A., Ehlers, T. A., Kühn, P., Kuzyakov, Y., Leinweber, P., Scholten, T., Spielvogel, S., Spohn, M.,  
.121 Übernickel, K., Tielbörger, K., Wagner, D., and Blanckenburg, F. von: Chemistry and microbiology of the Critical Zone along  
.122 a steep climate and vegetation gradient in the Chilean Coastal Cordillera, *CATENA*, 170, 183–203,  
.123 https://doi.org/10.1016/j.catena.2018.06.002, 2018.
- .124 Rengers, F. K., McGuire, L., Kean, J. W., Staley, D. M., and Hobley, D. E. J.: Model simulations of flood and debris flow  
.125 timing in steep catchments after wildfire, *Water Resour. Res.*, 52, 6041–6061, https://doi.org/10.1002/2015WR018176, 2016.
- .126 Rodell, M., Houser, P. R., Jambor, U., Gottschalck, J., Mitchell, K., Meng, C.-J., Arsenault, K., Cosgrove, B., Radakovich, J.,  
.127 Bosilovich, M., Entin, J. K., Walker, J. P., Lohmann, D., and Toll, D.: The Global Land Data Assimilation System, *Bull. Am. Meteoro  
.128* Soc., 85, 381–394, https://doi.org/10.1175/BAMS-85-3-381, 2004.
- .129 Schaller, M. and Ehlers, T. A.: Comparison of soil production, chemical weathering, and physical erosion rates along a climate  
.130 and ecological gradient (Chile) to global observations, *Earth Surf. Dyn.*, 10, 131–150, https://doi.org/10.5194/esurf-10-131-  
.131 2022, 2022.
- .132 Schaller, M., Ehlers, T. A., Lang, K. A. H., Schmid, M., and Fuentes-Espoz, J. P.: Addressing the contribution of climate and  
.133 vegetation cover on hillslope denudation, Chilean Coastal Cordillera ( $26^{\circ}$ – $38^{\circ}$ S), *Earth Planet. Sci. Lett.*, 489, 111–122,  
.134 https://doi.org/10.1016/j.epsl.2018.02.026, 2018.
- .135 Schaller, M., Dal Bo, I., Ehlers, T. A., Klotzsche, A., Drews, R., Fuentes Espoz, J. P., and van der Kruk, J.: Comparison of  
.136 regolith physical and chemical characteristics with geophysical data along a climate and ecological gradient, Chilean Coastal  
.137 Cordillera (26 to 38°S), *SOIL*, 6, 629–647, https://doi.org/10.5194/soil-6-629-2020, 2020.
- .138 Schmid, M., Ehlers, T. A., Werner, C., Hickler, T., and Fuentes-Espoz, J.-P.: Effect of changing vegetation and precipitation  
.139 on denudation – Part 2: Predicted landscape response to transient climate and vegetation cover over millennial to million-year  
.140 timescales, *Earth Surf. Dyn.*, 6, 859–881, https://doi.org/10.5194/esurf-6-859-2018, 2018.
- .141 [Sharma and Ehlers: LandLab investigations into the seasonal effects of precipitation and vegetation change on catchment  
.142 erosion., https://doi.org/10.5281/zenodo.8033782, 2023.](#)

- 143 Sharma, H., Ehlers, T. A., Glotzbach, C., Schmid, M., and Tielbörger, K.: Effect of rock uplift and Milankovitch timescale  
144 variations in precipitation and vegetation cover on catchment erosion rates, *Earth Surf. Dyn.*, 9, 1045–1072,  
145 https://doi.org/10.5194/esurf-9-1045-2021, 2021.
- 146 Shobe, C. M., Tucker, G. E., and Barnhart, K. R.: The SPACE 1.0 model: A Landlab component for 2-D calculation of  
147 sediment transport, bedrock erosion, and landscape evolution, *Geosci. Model Dev. Discuss.*, 1–38,  
148 https://doi.org/10.5194/gmd-2017-175, 2017.
- 149 Starke, J., Ehlers, T. A., and Schaller, M.: Latitudinal effect of vegetation on erosion rates identified along western South  
150 America, *Science*, 367, 1358–1361, https://doi.org/10.1126/science.aaz0840, 2020.
- 151 Steegen, A., Govers, G., Nachtergaelie, J., Takken, I., Beuselinck, L., and Poesen, J.: Sediment export by water from an  
152 agricultural catchment in the Loam Belt of central Belgium, *Geomorphology*, 33, 25–36, https://doi.org/10.1016/S0169-  
153 555X(99)00108-7, 2000.
- 154 Stephenson, J., Gallagher, K., and Holmes, C.: A Bayesian approach to calibratingapatite fission track annealing models for  
155 laboratory and geological timescales, *Geochim. Cosmochim. Acta*, 70, 5183–5200, https://doi.org/10.1016/j.gca.2006.07.027,  
156 2006.
- 157 Suescún, D., Villegas, J. C., León, J. D., Flórez, C. P., García-Leoz, V., and Correa-Londoño, G. A.: Vegetation cover and  
158 rainfall seasonality impact nutrient loss via runoff and erosion in the Colombian Andes, *Reg. Environ. Change*, 17, 827–839,  
159 https://doi.org/10.1007/s10113-016-1071-7, 2017.
- 160 Tucker, G. E. and Bras, R. L.: A stochastic approach to modeling the role of rainfall variability in drainage basin evolution,  
161 *Water Resour. Res.*, 36, 1953–1964, https://doi.org/10.1029/2000wr900065, 2000.
- 162 [Tucker, G. E., Gasparini, N. M., Lancaster, S. T., and Bras, R. L.: Modeling Floodplain Dynamics and Stratigraphy: Implications for Geoarchaeology, 1999.](#)
- 163 Übernickel, K., Ehlers, T. A., Ershadi, M. R., Paulino, L., Fuentes Espoz, J.-P., Maldonado, A., Oses-Pedraza, R., and von  
164 Blanckenburg, F.: Time series of meteorological station data in the EarthShape study areas of the Coastal Cordillera, Chile,  
165 https://doi.org/10.5880/FIDGEO.2020.043, 2020.
- 166 Wang, L., Zheng, F., Liu, G., Zhang, X. J., Wilson, G. V., Shi, H., and Liu, X.: Seasonal changes of soil erosion and its spatial  
167 distribution on a long gentle hillslope in the Chinese Mollisol region, *Int. Soil Water Conserv. Res.*, 9, 394–404,  
168 https://doi.org/10.1016/j.iswcr.2021.02.001, 2021.
- 169 Wei, W., Chen, L., Zhang, H., and Chen, J.: Effect of rainfall variation and landscape change on runoff and sediment yield  
170 from a loess hilly catchment in China, *Environ. Earth Sci.*, 73, 1005–1016, https://doi.org/10.1007/s12665-014-3451-y, 2015.
- 171 Whipple, K. X. and Tucker, G. E.: Dynamics of the stream-power river incision model: Implications for height limits of  
172 mountain ranges, landscape response timescales, and research needs, *J. Geophys. Res. Solid Earth*, 104, 17661–17674,  
173 https://doi.org/10.1029/1999jb900120, 1999.
- 174 Wulf, H., Bookhagen, B., and Scherler, D.: Seasonal precipitation gradients and their impact on fluvial sediment flux in the  
175 Northwest Himalaya, *Geomorphology*, 118, 13–21, https://doi.org/10.1016/j.geomorph.2009.12.003, 2010.
- 176 Yetemen, O., Istanbulluoglu, E., Flores-Cervantes, J. H., Vivoni, E. R., and Bras, R. L.: Ecohydrologic role of solar radiation  
177 on landscape evolution, *Water Resour. Res.*, 51, 1127–1157, https://doi.org/10.1002/2014wr016169, 2015.
- 178 Zhang, S., Li, Z., Hou, X., and Yi, Y.: Impacts on watershed-scale runoff and sediment yield resulting from synergetic changes  
179 in climate and vegetation, *Catena*, 179, 129–138, https://doi.org/10.1016/j.catena.2019.04.007, 2019.
- 180 Zhang, W., An, S., Xu, Z., Cui, J., and Xu, Q.: The impact of vegetation and soil on runoff regulation in headwater streams on  
181 the east Qinghai-Tibet Plateau, China, *Catena*, 87, 182–189, https://doi.org/10.1016/j.catena.2011.05.020, 2011.
- 182 Zhang, X., Yu, G. Q., Li, Z. B., and Li, P.: Experimental Study on Slope Runoff, Erosion and Sediment under Different  
183 Vegetation Types, *Water Resour. Manag.*, 28, 2415–2433, https://doi.org/10.1007/s11269-014-0603-5, 2014.
- 184 Zheng, F. L.: Effect of Vegetation Changes on Soil Erosion on the Loess Plateau 1Project supported by the Chinese Academy  
185 of Sciences (No. KZCX3-SW-422) and the National Natural Science Foundation of China (Nos. 9032001 and 40335050),  
186 *Pedosphere*, 16, 420–427, https://doi.org/10.1016/S1002-0160(06)60071-4, 2006.
- 187

|188 Ziese, M., Rauthe-Schöch, A., Becker, A., Finger, P., Rustemeier, E., and Schneider, U.: GPCC Full Data Daily Version 2020  
|189 at 1.0°: Daily Land-Surface Precipitation from Rain-Gauges built on GTS-based and Historic Data: Gridded Daily Totals  
|190 (2020), [https://doi.org/10.5676/DWD\\_GPCC/FD\\_D\\_V2020\\_100](https://doi.org/10.5676/DWD_GPCC/FD_D_V2020_100), 2020.

|191